



Growth and reproduction of carpet shark, common electric ray and blind electric ray in New Zealand waters

New Zealand Aquatic Environment and Biodiversity Report No. 195

M.P. Francis
C. Ó Maolagáin
W.S. Lyon

ISSN 1179-5352 (online)
ISBN 978-1-77665-767-4 (online)

January 2018



Requests for further copies should be directed to:

Publications Logistics Officer
Ministry for Primary Industries
PO Box 2526
WELLINGTON 6140

Email: brand@mpi.govt.nz
Telephone: 0800 00 83 33
Facsimile: 04-894 0300

This publication is also available on the Ministry for Primary Industries websites at:
<http://www.mpi.govt.nz/news-and-resources/publications>
<http://fs.fish.govt.nz> go to Document library/Research reports

© Crown Copyright - Ministry for Primary Industries

TABLE OF CONTENTS

EXECUTIVE SUMMARY	1
1. INTRODUCTION	2
2. METHODS	3
2.1 Specimen and data collection	3
2.2 Vertebrae	3
2.3 Eye lenses	4
3. RESULTS	5
3.1 Specimens	5
3.2 Eye lens increments	6
3.3 Micro-CT scans	9
3.4 Carpet shark (CAR)	13
3.4.1 Introduction	13
3.4.2 Age and growth	13
3.4.3 Reproduction	17
3.5 Common electric ray (ERA)	19
3.5.1 Introduction	19
3.5.2 Age and growth	19
3.5.3 Reproduction	22
3.6 Blind electric ray (BER, TAY, TTA)	22
3.6.1 Introduction	22
3.6.2 Age and growth	23
3.6.3 Reproduction	26
4. DISCUSSION	28
5. MANAGEMENT IMPLICATIONS	32
6. ACKNOWLEDGMENTS	32
7. REFERENCES	32
APPENDIX 1: Reproductive staging guide for sharks and rays	36

EXECUTIVE SUMMARY

Francis, M.P.; Ó Maolagáin, C.; Lyon, W.S. (2018). Growth and reproduction of carpet shark, common electric ray and blind electric ray.

New Zealand Aquatic Environment and Biodiversity Report No. 195. 36 p.

The Ministry for Primary Industries (MPI) is developing a risk assessment framework to identify the nature and extent of risks to chondrichthyan populations. This project aims to fill some of the knowledge gaps for some of the high-risk, non-Quota Management System species to reduce the level of uncertainty in the risk assessments of those species, and to provide information on their productivity that can then be used as inputs into future quantitative risk assessments. The species included in this study were carpet shark, *Cephaloscyllium isabellum*, common electric ray, *Tetronarce nobiliana*, and blind electric ray, *Typhlonarke aysoni*. Specimens and data were collected aboard commercial fishing vessels and research vessels, and integrated with existing data and specimens held by NIWA.

All three species were aged by counting growth bands on their vertebrae, either under reflected white light (common electric ray) or after X-raying (carpet shark and blind electric ray). Common electric ray and carpet shark were also aged by estimating the number of micro-increments deposited in their eye lenses between birth and capture, and dividing by 365 (based on an assumption that one micro-increment is formed per day). Samples sizes were mostly small and vertebral bands were unclear so the results presented here are regarded as preliminary and uncertain, but are the best available for these species. Age estimates from vertebrae exceeded those from eye lenses by factors of five for carpet shark and six for common electric ray. Since neither ageing method has been validated for these species, we cannot say which, if either, is correct. However, the vertebral ages are regarded as more plausible, and they indicate that all three species grow moderately fast, reaching maturity at about 2 years for male common rays and both sexes of blind electric rays, and 5–9 years for carpet shark. Longevity is low to moderate, compared with other elasmobranchs, being 5–10 years for males and 10–16 years for females.

Carpet shark males mature at about 60 cm total length (TL) and females at 76 cm TL. Egg-laying occurs year-round, and the time to hatching after deposition of eggs in an aquarium was about 12–14 months. Length at hatching is about 16–17 cm TL. Our samples provided few useful data on reproduction in common electric rays. The length at maturity is about 60 cm TL for males, and possibly around 90 cm TL for females, although there is conflicting evidence about the latter. Other aspects of reproduction in common electric rays are totally unknown in New Zealand or Australian waters. In the Atlantic Ocean and Mediterranean Sea, *T. nobiliana* females grow larger than males (120 cm TL versus 75 cm TL); gestation lasts one year and there is no concurrent ovarian egg development, suggesting that birth is followed by a resting period and that the reproductive cycle may be two years long; birth occurs at 17–25 cm TL; litter size is as high as 60; and fecundity increases with the size of the mother. Considerable new information was available on reproduction of blind electric rays. Median length at sexual maturity was 20–21 cm TL for both sexes, although the confidence intervals were relatively wide. Nine pregnant females were found, providing the first litters to be reported since 1909. Litter size probably averages less than 10 embryos, with a maximum of 11. The length at birth is 10 cm TL. No information is available on the length of the gestation period or whether females have a resting period between pregnancies. Males and females appear to reach similar maximum lengths, with a 43.4 cm male reported in this study being the largest specimen yet recorded.

Some reproductive parameters remain unknown, uncertain, or are derived from overseas populations that may differ from New Zealand. In particular, the length of the gestation period and whether females have a resting period between pregnancies are poorly known or unknown for the two electric rays, as is the number of eggs laid annually by carpet sharks. Uncertainty about these parameters would have a big effect on productivity estimates.

1. INTRODUCTION

One of the major goals of the New Zealand National Plan of Action for the Conservation and Management of Sharks (NPOA-Sharks) is to ‘Maintain the biodiversity and long-term viability of New Zealand shark populations based on a risk assessment framework with assessment of stock status, measures to ensure any mortality is at appropriate levels, and protection of critical habitat’ (Ministry for Primary Industries 2013). The Ministry for Primary Industries (MPI) is developing a risk assessment framework to identify the nature and extent of risks to chondrichthyan populations through expert-based and quantitative methods. The first step in that process was in November 2014 when MPI convened an expert panel to conduct a qualitative risk assessment of all New Zealand cartilaginous fishes (Ford et al. 2015). That risk assessment ranked New Zealand’s chondrichthyan species by their perceived risk, and identified gaps in our knowledge of the biological productivity of each species. The present project aims to fill some of the knowledge gaps for some of the high-risk, non-Quota Management System (QMS) species in order to reduce the level of uncertainty in the risk assessments of those species, and to provide information on their productivity that can then be used as inputs into future risk assessments.

The Overall Research Objective of the present study was: *To estimate basic biological parameters for high risk, high uncertainty chondrichthyans.*

There were three Specific Research Objectives:

1. *To collect (from observers and/or research trawls, or other sources) and store specimens for selected chondrichthyan species.*
2. *To test the efficacy of potential ageing techniques on a subset of specimens for each species collected.*
3. *To process specimens for ageing and other biological parameters, reliant on the outcome of Objectives 1 and 2 and in consultation with MPI.*

The species included in this study were three rays and five sharks (with MPI three-letter species codes):

1. **Common electric ray, *Tetronarce nobiliana* (ERA)**
2. **Blind electric ray, *Typhlonarke aysoni* (BER, TAY)**
3. **Blind electric ray, *Typhlonarke tarakea* (BER, TTA)**
4. **Carpet shark, *Cephaloscyllium isabellum* (CAR)**
5. Seal shark, *Dalatias licha* (BSH)
6. Longnose velvet dogfish, *Centroselachus crepidater* (CYP)
7. Plunket’s shark, *Scymnodon plunketi* (PLS)
8. Owston’s dogfish, *Centroscymnus owstonii* (CYO)

These eight species all fall within the top 11 non-QMS elasmobranch species having the greatest risk in the qualitative risk assessment (Ford et al. 2015). In this report, we deal with the first four species listed (in bold) above; the remaining four species are covered by Francis et al. (2018). The two blind electric rays are treated here as one species (see Section 3.6.1).

All eight species are caught as unintended bycatch by trawlers, and to a lesser extent by other fishing methods, around New Zealand. Specimens and data were collected to estimate age, growth, longevity, length and age at maturity, and reproductive parameters (including, where possible, gestation period, fecundity, and length at birth). Collections were made by observers aboard commercial fishing vessels, and by scientists aboard research vessels. These new specimens and data were integrated with existing data and specimens held by NIWA.

2. METHODS

2.1 Specimen and data collection

This project proceeded in two main phases. Phase 1 consisted of the collection of small numbers of specimens of each species, and experimental processing of various hard parts to determine the best structure and technique for revealing growth bands. Phase 2 consisted of the collection of larger samples of the most useful ageing structures, and processing and ageing those samples using the best technique(s).

In Phase 1, specimens were collected mainly by scientists during research voyages on RVs *Tangaroa* and *Kaharoa*. In Phase 2, MPI observers, in addition to scientists, were requested to collect larger numbers of specimens, and maturity-stage data. Most specimens and new data were collected between April 2015 and August 2017. Forty-three additional specimens of blind electric ray were available from opportunistic collections of specimens, coordinated by M. Francis, from trawl surveys conducted between 2008 and 2014. Most specimens came from around the South Island and adjacent plateaux (Chatham Rise, Campbell Plateau). In the rest of this report, results from both Phase 1 and Phase 2 are combined, but most of the shark and ray ages came from Phase 2 samples.

Hard parts tested for suitability for ageing during Phase 1 were vertebrae and eye lenses. In Phase 2, both vertebrae and eye lenses were used for estimating the ages of carpet shark and common electric ray. Blind electric rays have vestigial eyes buried beneath the skin, and lack eye lenses (Phillipps 1929; Garrick 1951, 1952), so only vertebrae were used for ageing this species. Lenses and vertebrae were usually removed from carpet sharks at sea, whereas common and blind electric rays were usually brought back to the laboratory whole and sampled there. All samples were dissected out in NIWA's ecology containment laboratory using aseptic techniques.

Carpet sharks were measured for total length (TL), common electric rays for pelvic length (PL), and blind electric rays for both. Reproductive data were collected during research and observer trips, with maturity stages being assigned to sharks and rays using the staging scheme shown in Appendix 1. Size and reproductive data collected on research voyages before April 2015 were extracted from the MPI *trawl* database and combined with the data collected for this project.

2.2 Vertebrae

Band counts on vertebrae are widely used for age estimation in elasmobranchs, with vertebrae viewed either whole or following sectioning to about 0.5 mm thickness, and sometimes stained to enhance band clarity.

A block of 3–7 vertebrae was dissected from each specimen and frozen. In the laboratory, vertebral blocks were defrosted, a few of the largest visible vertebrae were removed, and physically trimmed of connective tissue and residual neural and haemal arches. The vertebral centra were then bleached for about 15 minutes in sodium hypochlorite to remove connective tissue. Whole, half and thick-sectioned vertebrae were examined under reflected and transmitted light. Small subsamples of whole vertebrae were processed further by bisecting them through the focus in the transverse plane (Wilson et al. 1987), and mounting one or both half-centra, conical side downwards, with double-sided tape on to a plastic transparency sheet. These subsamples were then X-rayed at 50 kV and ~5 mA at various exposure times onto Industrex M100 X-ray film, and the developed films were examined under a stereomicroscope.

Selected frozen whole vertebrae were imaged in a micro-computed tomography (micro-CT) machine Skyscan 1172 at the University of Otago, Dunedin. Micro-CT uses X-ray technology to produce image slices through objects, which can be reconstructed into virtual, 3-dimensional images that can be rotated and viewed in any orientation (Geraghty et al. 2012). The settings used for the micro-CT scanner were: source voltage 40 kV, image pixel size 17.34 μm , no filter, rotation step 0.40°, frame averaging on=4, random movement on=4. The scanning time for each sample was about 30 minutes. Data files were

post-processed with ImageJ (Abramoff et al. 2004), using associated 3D plugin routines that provided both serial sections and video animations for further analysis.

Each pair of opaque and translucent vertebral bands was counted as a ‘band pair’, hereafter referred to simply as a band. Shark and ray species often display a ‘birth band’, which is a prominent contrasting band in the centrum deposited about or soon after birth. Identification of this band is important in order to determine where subsequent band counts should begin. However, too few newborn individuals or embryos were available for us to identify the location of the birth band, so all visible bands were counted, and then adjusted empirically for the birth band after inspection of the results (see below).

One reader (M. Francis) carried out an initial ‘familiarisation’ read of all vertebrae while knowing the lengths of the specimens. At two later dates, the same reader made additional blind readings of all vertebrae, without knowing the lengths of the specimens. These last two readings were averaged to generate a mean age estimate for each specimen. Ideally, we would have used a second reader to enable estimation of between-reader variability. However, because of the number of species covered by both parts of this project, and the time-consuming nature of the methodology testing in Phase 1 and specimen preparation, it was only practical to use one reader. Consequently, results presented here are regarded as provisional and they require further corroboration and validation.

Vertebral readings 1 and 2 were plotted against each other to check for consistency of age estimates. Small sample sizes meant that statistical analyses were not warranted. Growth curves were fitted to the length-at-mean-age data using the R package FSA (version 0.1.7) (R Development Core Team 2008), which fits non-linear curves using the R package nlstools. The von Bertalanffy growth model was used:

$$L_t = L_\infty \left(1 - e^{-K[t-t_0]}\right)$$

where L_t is the expected length at age t years, L_∞ is the asymptotic maximum length, K is the Brody growth coefficient, t is the fish age in years, and t_0 is the theoretical age at zero length. The data were inspected for growth differences between males and females, but sample sizes were too small to test for significant differences between male and female growth curves.

2.3 Eye lenses

Eye lenses grow within a fluid/gel-filled capsule, in much the same way that fish otoliths grow. Hence, they may continue to grow independently of body size after somatic growth has ceased. This potentially provides a structure from which age estimates can be obtained. Ageing may involve measuring lens weight or diameter and identifying modal peaks and troughs that may represent year classes (Crivelli 1980; Douglas 1987; Siezen 1989; Francis & Ó Maolagáin 2001). An alternative technique, trialled in cephalopods but not, as far as we are aware, in fishes, is to enumerate micro-increments present in the eye lens cores (Baqueiro Cárdenas et al. 2011; Rodríguez-Domínguez et al. 2013). This method relies on the assumption that the lens micro-increments are deposited daily.

Both eye lenses were removed whole by scientists and observers at sea, and stored frozen until preparation. After defrosting, the crystalline eye lens cores were removed, blotted dry, the diameter of one randomly chosen core was measured with a digital micrometer, and selected cores were embedded in epoxy, and then cut in half with a diamond saw. Half lenses were adhered onto microscope slides with thermoplastic resin and ground and polished until micro-increments became visible under a compound microscope using transmitted light. Because of the large number of micro-increments visible under high magnification, and the fact that it was rarely possible to see increments across the entire lens section, counting a full complement of increments on each section was impractical. Instead, digital images were taken of increments, and average increment width measurements were made at a range of different distances between the focus and the lens margin using calibrated ImageJ software. The number of increments used to estimate average increment width depended on how many were visible at a particular location: it ranged from 3 to 40 increments (mean 15.4), but was usually 10–40 (85% of measurements). The lens cores used for age estimation are hereafter referred to as eye lenses.

Lens-based age estimates were derived for carpet shark and common electric ray by estimating the number of increments laid down between birth and death as follows:

1. A linear regression was fitted to a plot of eye lens diameter versus TL or PL.
2. The linear regression was extrapolated backwards to the length at birth to produce an estimate of the lens diameter at birth. The values of length at birth used were: carpet shark 16 cm TL (Section 3.4.1), and common electric ray 17 cm PL (estimated as 0.73 x 23 cm TL; Section 3.5.1).
3. Lens diameter at birth was halved to give the estimated lens radius at birth.
4. Lens diameters at death (i.e., when sampled) were corrected for 'shrinkage' during sectioning (see Section 3.2) and halved to give lens radius at death.
5. Exponential curves were fitted to plots of log(increment width) versus log(distance from lens focus) and used to predict increment width at any given distance from the focus:

$$\log_{10}(\text{increment width}) = a - b * \exp(-c * (\log_{10}(\text{distance from focus})))$$

6. The number of increments formed between birth and death was estimated by numerical integration of the exponential curve derived in step 5, between the radius at birth and the radius at death, using the R function *integrate*.
7. The age of each fish (in years) at death was calculated by dividing the number of increments estimated in step 6 by 365 (assuming one increment is formed per day).

3. RESULTS

3.1 Specimens

A total of 150 carpet sharks, 16 common electric rays, and 141 blind electric rays were available for sampling (Table 1). Most of them provided vertebrae, but a few were missing length and sex data, and many blind electric rays were received after vertebral processing had been completed, so fewer animals were available for ageing. Because of the increased preparation and processing time required, only small subsamples of vertebrae (12–18 per species) were X-rayed. For carpet shark and common electric ray, average eye lens increment widths were measured for a few animals at several locations across the lens (Table 1). Eye lens diameters were measured for larger samples of lenses, and converted into estimated ages using the fitted relationships between increment width and distance from the focus (see Section 3.2).

The sampled carpet sharks were mainly sub-adults and adults, with most sharks exceeding 60 cm TL (Figure 1). Common electric rays proved to be uncommon and were rarely sampled; however, the females collected covered a wide length range. The entire length range of blind electric rays was sampled, ranging from a 10.5 cm TL newborn to a 43.4 mm TL male, the largest *Typhlonarke* ever recorded. Because this large specimen was valuable as a museum voucher specimen, it was not sampled for vertebrae.

Table 1: Number of specimens of three species used for ageing. NA = not available.

	Total specimens	Whole vertebrae	X-rayed vertebrae	Eye lens increment widths	Eye lens diameters	Eye lens ages
Carpet shark (CAR)	150	143	18	14	107	107
Common electric ray (ERA)	16	14	12	5	10	10
Blind electric ray (BER)	141	94	18	NA	NA	NA

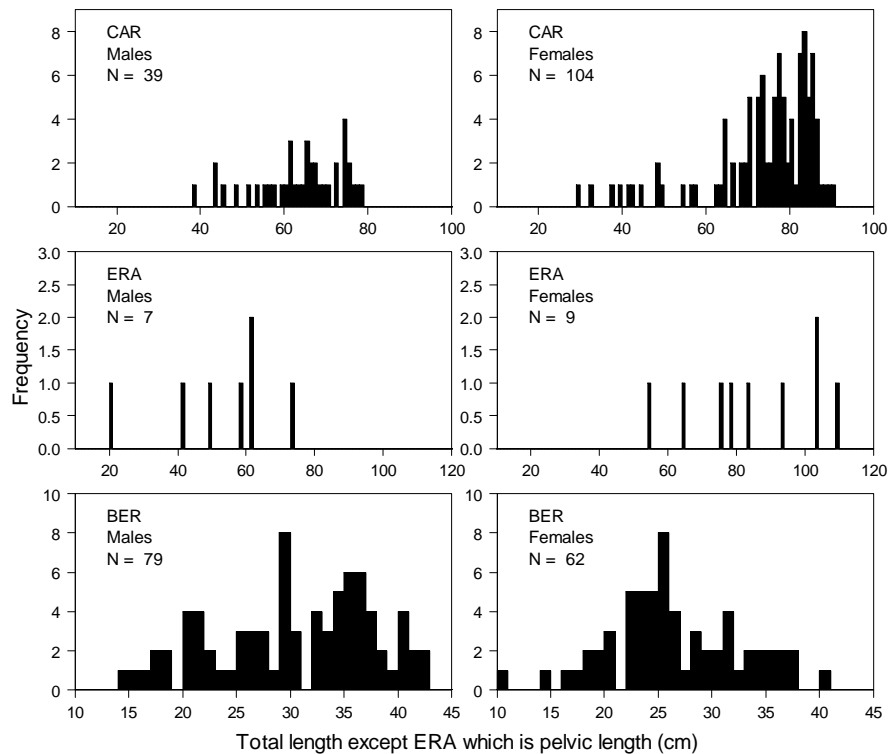


Figure 1: Length-frequency distributions of the specimens collected during the present study. CAR, carpet shark; ERA, common electric ray; BER, blind electric ray. Sample sizes are smaller for carpet shark than indicated in Table 1 because a few specimens lacked length or sex data.

3.2 Eye lens increments

Fish eye lenses are spherical and are composed of concentric protein layers (Fernald 1985). Lens diameter was positively correlated with TL for carpet shark and PL for common electric ray (Figure 2). There was considerable variability among fish, which for carpet shark may have been related to gender, with males and females separating slightly. However, we used a single regression relationship for both sexes combined in subsequent analyses. Estimated lens diameters at birth were 1.22 mm for carpet shark and 1.68 mm for common electric ray (Table 2).

The concentric layers in the eye lens are not strongly bound, and some of the layers ‘fractured’ apart because of the physical stress involved in sectioning and grinding (Figure 3A–C, E). Major fracture zones were apparent around the entire lens, but much shorter partial fractures were often only apparent at high magnification. There was no reduction in increment width before or after the fractures (Figure 3B, C), so they do not appear to represent zones of reduced increment growth that might occur in periods of slow somatic growth, such as during winter. We assumed that no increments were ‘lost’ at fracture zones. The same is not true for the outer surface of the lens. Before sectioning, the gelatinous outer surface was gently blotted dry to facilitate subsequent embedding in resin. Microscopic examination of the outer edge of sections indicated that the gelatinous surface layer comprised delicate sheets of newly formed or forming micro-increments that were broken or lost during sectioning. We could not estimate the number of micro-increments that were lost this way, but we believe it was a few percent or less of the total number of increments. No correction was made for the resulting underestimation of age.

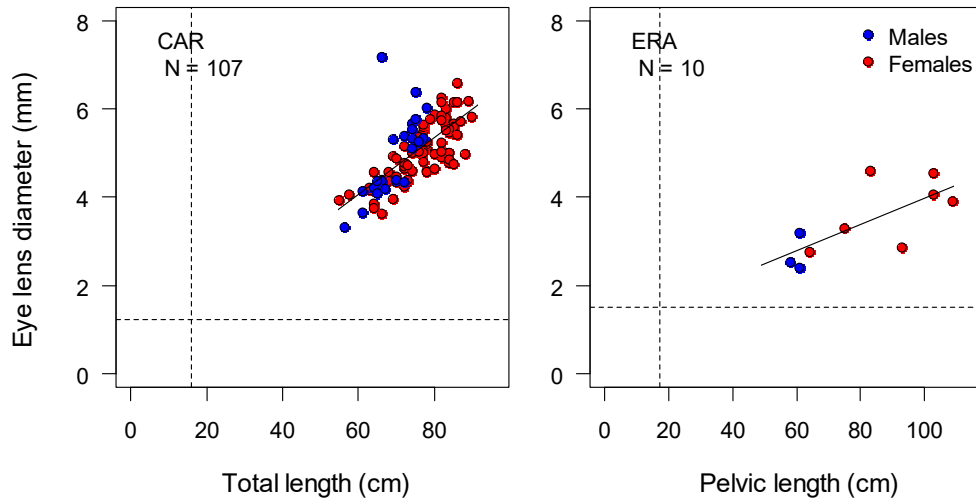


Figure 2: Relationship between eye lens diameter and total length for carpet shark (CAR) and common electric ray (ERA). The vertical dashed line is the length at hatching (CAR) or birth (ERA), and the horizontal dashed line is the eye lens diameter at hatching or birth calculated by backwards extrapolation of the regression line. Linear regression parameters are provided in Table 2.

Table 2: Eye lens core measurements for carpet shark (CAR) and common electric ray (ERA). Regression parameters are also provided for the linear regressions fitted to the data in Figure 2, and the curves fitted to the data in Figure 5 using the equation: $\log_{10}(\text{increment width}) \sim a - b * \exp(-c * (\log_{10}(\text{distance from focus})))$.

	Species	
	CAR	ERA
Length at birth (cm)	16	17*
Lens diameter at birth (mm)	1.22	1.68
Standard error (mm)	0.38	0.61
Lens radius at birth (mm)	0.61	0.84
Lens maximum diameter (mm)	7.17	4.59
Linear regression parameters from Figure 2		
<i>a</i>	0.196	0.998
<i>b</i>	0.064	0.030
R^2	0.490	0.471
Non-linear regression parameters from Figure 5		
<i>a</i>	0.9061	0.6774
<i>b</i>	0.1531	0.0124
<i>c</i>	-0.4852	-1.1492
R^2	0.639	0.491

* Pelvic length

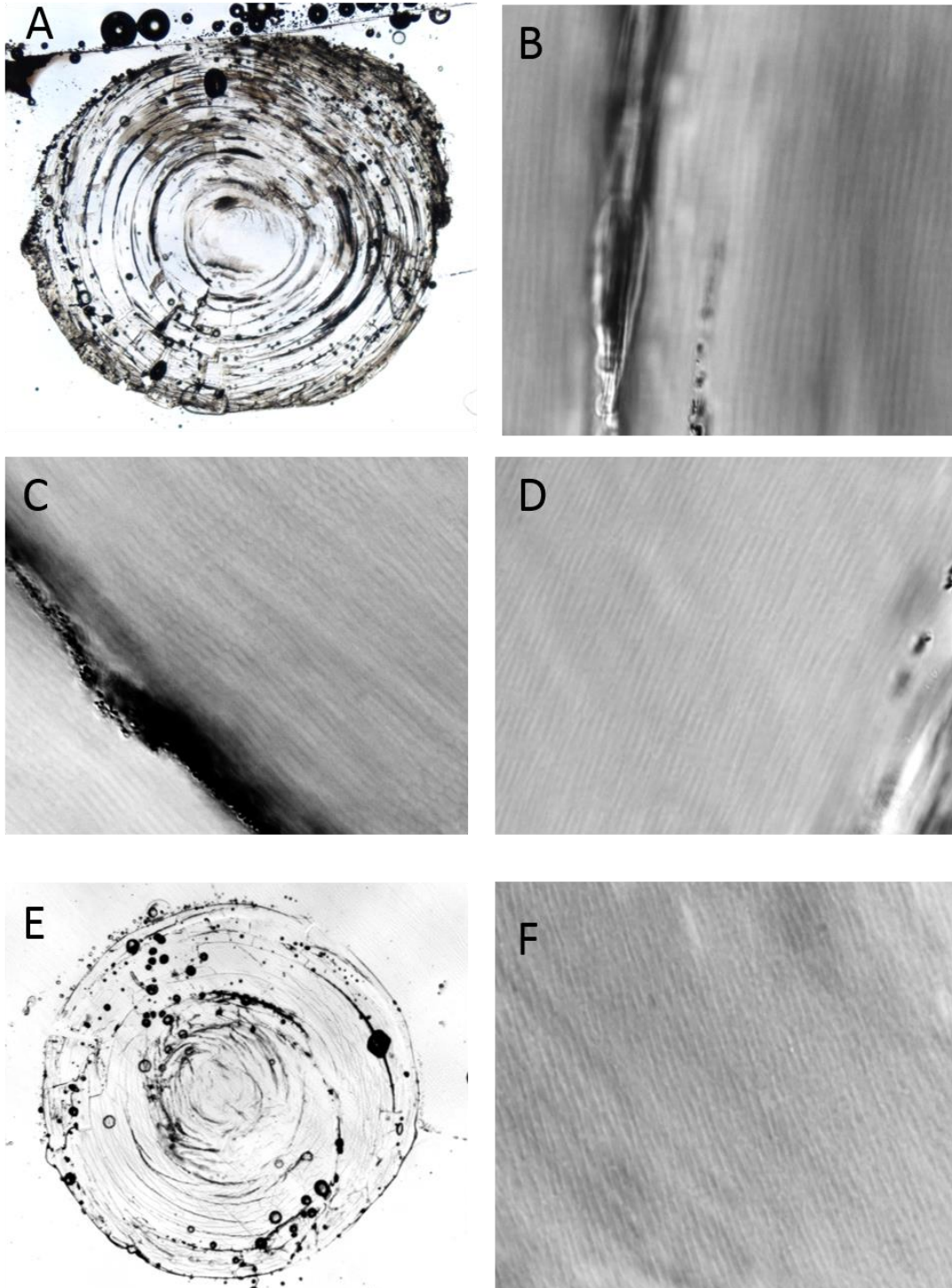


Figure 3: Whole-lens sections and high magnification images of eye lens micro-increments in carpet shark (A–D) and common electric ray (E–F). A, B: CAR 26, 57 cm TL female, lens diameter 4.1 mm, increments c. 1.9 μ m wide. C: CAR 29, 54 cm TL female, increments c. 2.0 μ m wide. D: CAR 30, 56 cm TL male, increments c. 1.9 μ m wide. E, F: ERA 4, 75 cm PL female, lens diameter 3.3 mm, increments c. 1.9 μ m wide.

Nevertheless, we observed ‘shrinkage’ of the eye lens between the whole and sectioned states (Figure 4). Shrinkage was consistent across the six species analysed in this study and by Francis et al. (2018), and because each species was represented by only a few specimens, and each species had different-sized eye lenses, we combined all species when estimating the amount of shrinkage (Figure 4). The slope of the relationship between section diameter and whole-lens diameter was not significantly different from 1 (1.001 ± 0.017 , estimate ± 1 standard error), and section diameters were 0.263 mm (± 0.148 mm) smaller than whole diameters overall. Whole-lens diameters were subsequently converted to section diameters using this regression for analyses and plots involving comparisons of distances measured on lens sections. Median shrinkage across all species was 2.5%, but median shrinkages for carpet shark and common electric ray were 3.8% and 10.3%, respectively. The high value for common electric ray may be a result of the fact that it had the smallest eye lenses of all species examined. Lens shrinkage probably results from a combination of the loss of the newly formed outer layer of increments, and artefacts of the sectioning process.

Micro-increment widths declined between the focus and the outer margin (Figure 5). Increment width varied between 0.79 μm and 3.06 μm for carpet shark, and between 0.96 μm and 3.39 μm for common electric ray. The parameters of the exponential curves fitted to the data in Figure 5 are shown in Table 2. Residuals plots showed that the curves fitted the data reasonably well, although there was considerable variability, and the variance increased with lens size for common electric ray (albeit based on a small sample size of five rays).

3.3 Micro-CT scans

Micro-CT scans of vertebrae from carpet shark, common electric ray and blind electric ray are shown in Figure 6. Growth bands were visible in most specimens, but were sometimes faint (some of the better examples are shown in Figure 6). A big advantage of the micro-CT scans was the ability to digitally section a vertebra, rotate it in any orientation, and view an animated video of the vertebra rotating in three dimensions. These features often enhanced the appearance of the growth bands. They also revealed the presence of bands in the isthmus between two cones in a vertebra (see light-coloured central portion of Figure 6B). Micro-CT scans and conventional X-rays revealed similar numbers of bands (although for practical reasons, direct comparisons on the same shark or ray were not made). Conventional X-rays were easier, faster and cheaper to generate in our laboratory, so we used that method rather than micro-CT for ageing sharks and rays (see below). Nevertheless, micro-CT imaging has utility in revealing the structure of hard parts and the growth bands in preliminary studies using small samples of animals.

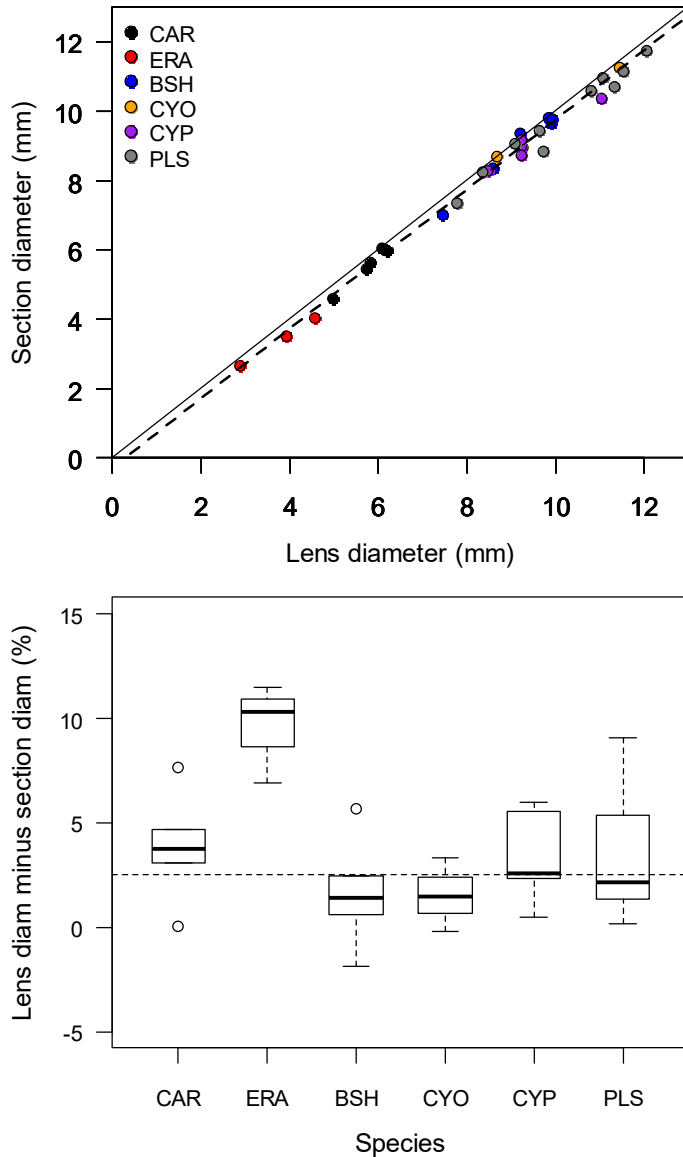


Figure 4: Top: Relationship between eye lens core diameter and eye lens section diameter for the same specimens. Bottom: Percentage differences between section diameter and lens diameter. The central black bar is the median, the box spans the first to third quartiles, and the whiskers extend to the most extreme data point, which is no more than 1.5 times the interquartile range from the box. CAR, carpet shark; ERA, common electric ray; BSH, seal shark; CYO, Owston’s dogfish; CYP, longnose velvet dogfish; PLS, Plunket’s shark. The horizontal dashed line indicates the median shrinkage across all six species (2.5%).

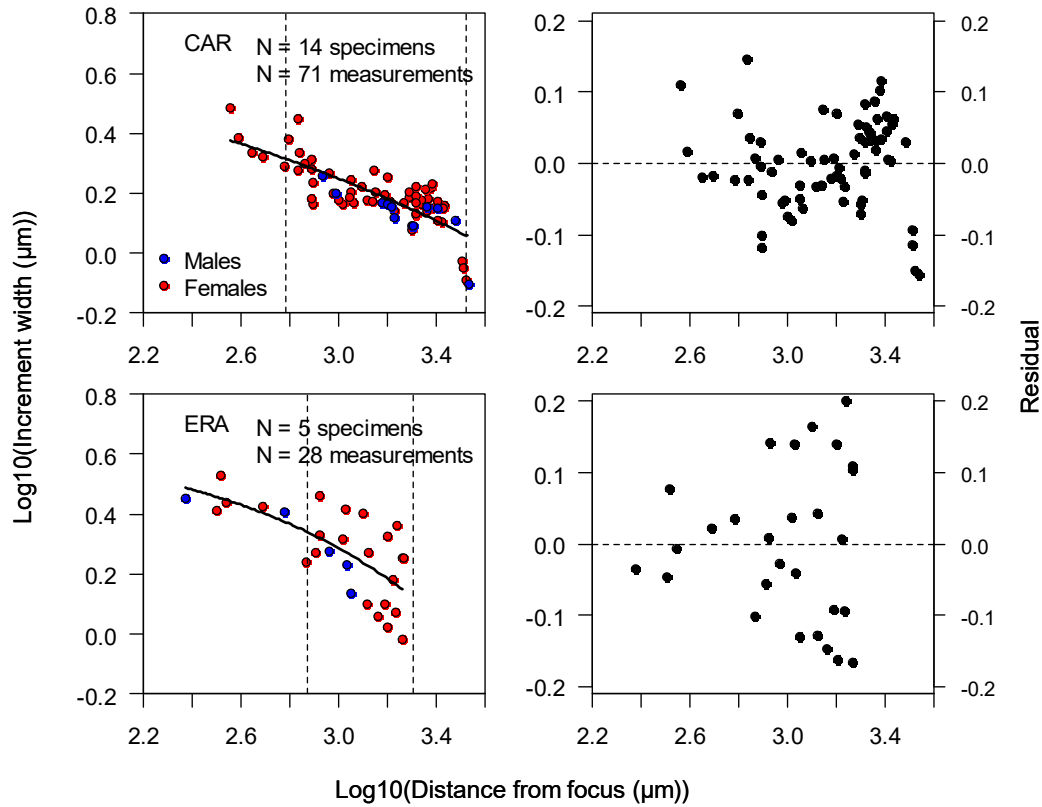


Figure 5: Relationship between the average width of eye lens micro-increments and the distance from the lens focus for carpet shark (CAR, top) and common electric ray (ERA, bottom). Non-linear regression curves were fitted to the data using the equation: $\log_{10}(\text{increment width}) \sim a - b * \exp(-c * (\log_{10}(\text{distance from focus})))$. Residuals are plotted in the right panels, and regression parameters are provided in Table 2. Vertical dashed lines in the left panels indicate the radius of the lens core at birth or hatching (left line) and the maximum lens radius observed (right line). The distance from the focus of one carpet shark measurement slightly exceeded the maximum lens radius because of the use of different measurement techniques: the distance from the focus was measured on a section under a microscope, and the lens radius was measured on a whole-lens core with callipers.

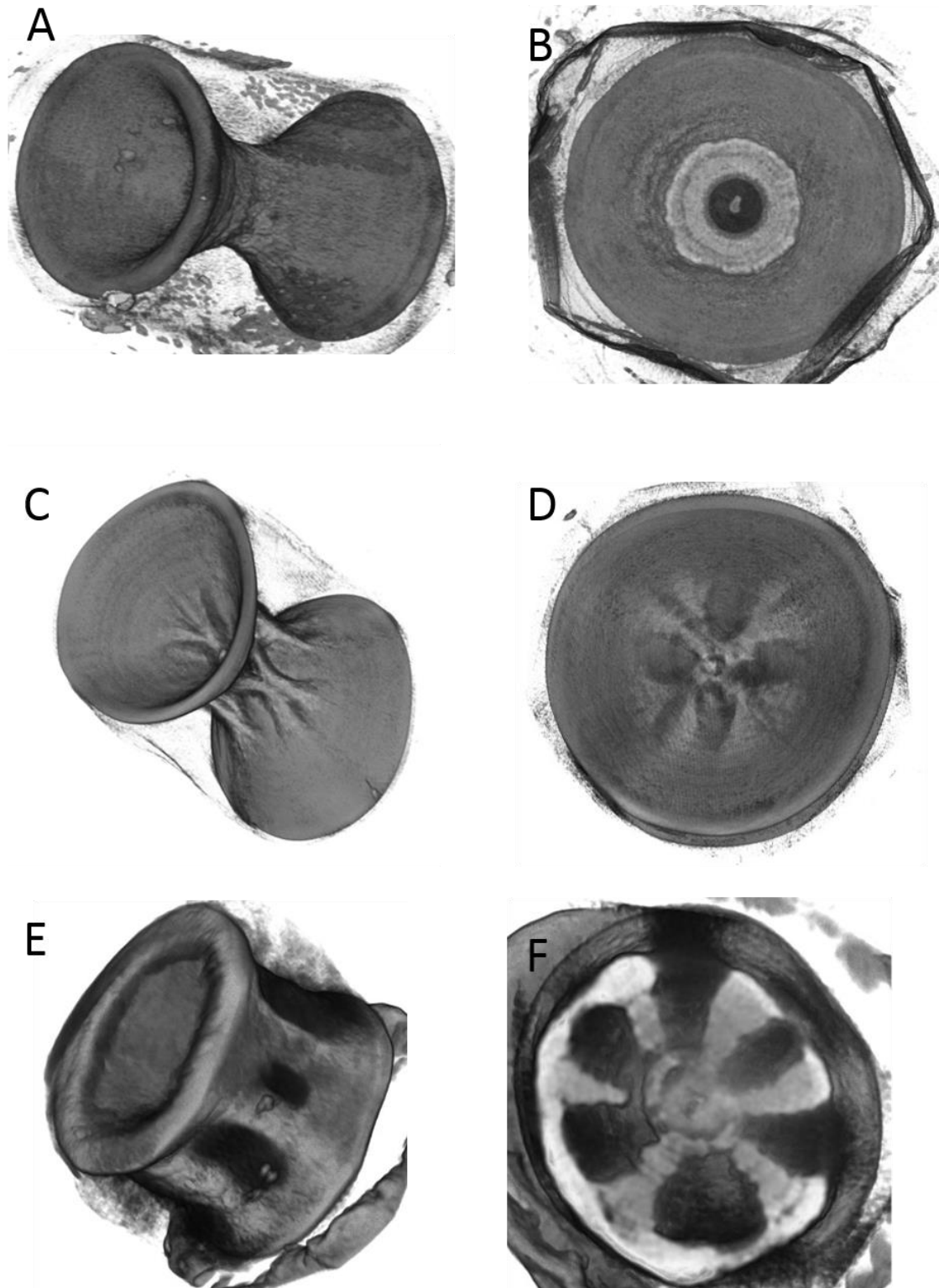


Figure 6: Micro-CT scans of whole vertebral centra (left) and half-centra viewed from the focus (right). A, B: Carpet shark CAR 26, 57 cm TL female. C, D: Common electric ray ERA 4, 75 cm PL female. E, F: Blind electric ray BER 2, 30 cm TL male.

3.4 Carpet shark (CAR)

3.4.1 Introduction

The carpet shark (*Cephaloscyllium isabellum*) is common in coastal waters around New Zealand (Anderson et al. 1998; Francis 2012; Nakaya et al. 2015; Horn 2016). A related species, *Cephaloscyllium* cf. *variegatum*, has been recorded from northern New Zealand based on only five specimens, four of which came from the Kermadec and Norfolk ridges, and one from the Bay of Plenty (Nakaya et al. 2015). All specimens used in this study came from south of Cook Strait so no confusion with the rare northern species is considered likely.

There have been no previous studies of the age and growth of carpet shark. Horn (2016) noted that length-frequency distributions of carpet sharks caught during trawl surveys showed no modal structure that might correspond with age classes, and concluded that either there is no strong seasonality in breeding, or that growth is slow or variable. Horn (2016) reviewed growth and tagging studies on other species of *Cephaloscyllium* and gave the following summary:

‘Short-term tagging studies of *C. umbratile* (a species with a maximum length similar to *C. isabellum*) held in aquaria in Japan showed that fish c. 25–35 cm TL had average monthly growth increments of about 3 mm in summer 1984 and 1985 and 17 mm in winter 1986, although shark mortality rates were high in all trials with few surviving more than 4 months (Tanaka 1990). However, these data infer growth of c. 12 cm per year for sharks that were probably in their first year following hatching. Taniuchi (1988) concluded (without providing evidence) that *C. umbratile* grew very slowly after maturity. The only located study that attempted to develop growth parameters for any *Cephaloscyllium* species was by Bell (2012) who aged Australian white-fin swell sharks (*C. albipinnum*) by counting zones on the surface of vertebrae. This species reached its asymptotic length (c. 1.1 m) and sexual maturity at 8–13 years and had a maximum age of c. 20 years. Bell (2012) noted, however, that the ageing method was not validated, and interpretation of the vertebral zones was difficult, but also commented that similar vertebral zonation was present for *C. laticeps*. Tag return data showed that *C. laticeps* can live for at least 7 years (Awruch et al. 2012).’

Carpet sharks are oviparous, laying two large leathery eggs at a time (Waite 1909; Graham 1956; Francis 2012). Length at hatching is about 16 cm TL (Waite 1909; Francis 2012; Nakaya et al. 2015). Length at 50% maturity is about 60 cm TL for males and 76 cm TL for females (Francis 2012; Nakaya et al. 2015; Horn 2016).

3.4.2 Age and growth

Length-frequency distributions of male and female carpet sharks sampled during west coast South Island (WCSI) trawl surveys in March–April and east coast South Island (ECSI) trawl surveys in May–June are shown in Figure 7. The WCSI plots include most of the carpet sharks plotted by Horn (2016), except with all surveys combined. Even though each survey series was restricted to a two-month period, there is no indication of modal structure for WCSI, and the modes present for ECSI males may be an artefact of the small sample size. Thus, we concur with Horn that there is no indication of age classes present in the length data.

In Phase 1, carpet shark vertebrae were observed to have growth bands on the surface of the centra cones, when viewed under reflected light (Figure 8A, B). Faint bands were also occasionally visible in thick sections (Figure 8C, lower left). Consequently, vertebrae from many specimens were cleaned in preparation for viewing whole. However, bands were found to be inconsistent, both within and between specimens, and we were unable to age large samples by this technique.

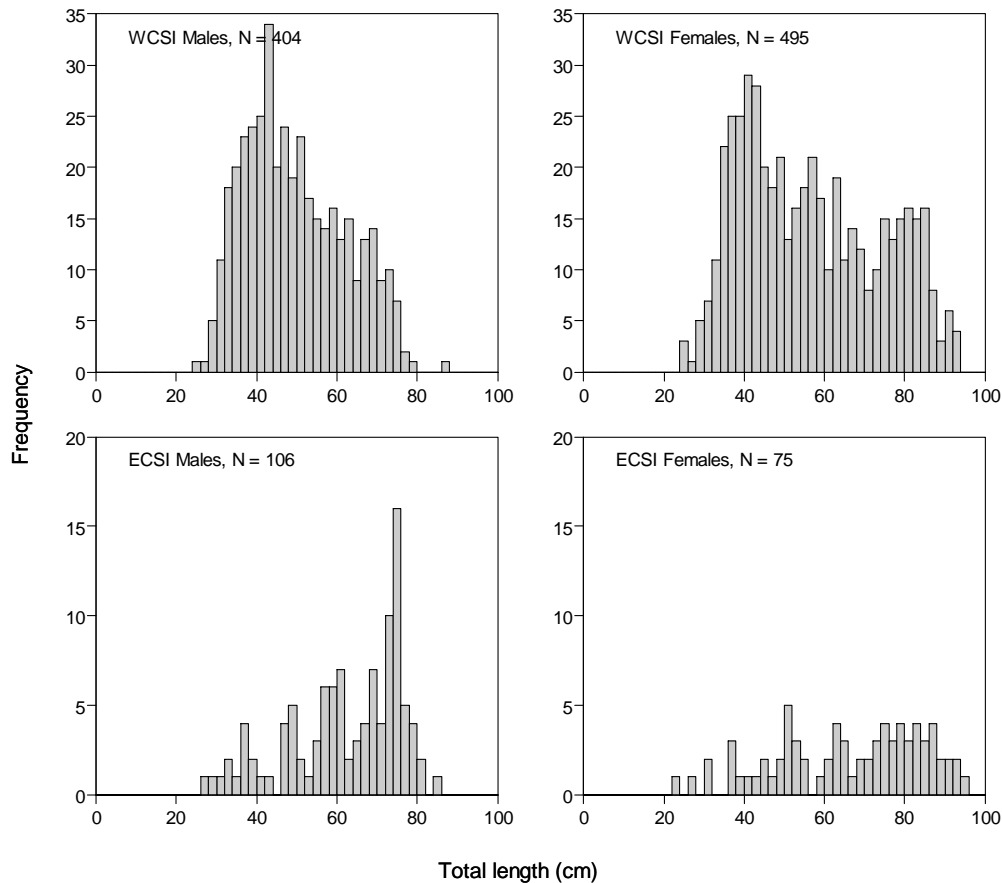


Figure 7: Length-frequency distributions by sex for carpet shark sampled during west coast South Island (WCSI) trawl surveys in March–April (top panels) and east coast South Island (ECSI) trawl surveys in May–June (bottom panels).

Instead, we X-rayed a subsample of vertebrae and used them for ageing. Growth bands were visible in most X-rays, but they were far from clear and age estimates were uncertain. Bands were sometimes visible in the isthmus (pale central portion of Figure 8D), and are analogous to the isthmus bands revealed by micro-CT scanning (Figure 6B), but were usually fewer in number than those visible on the centrum cone. We counted the cone latter bands (see Figure 8E, F) and used the band counts as age estimates.

The repeat readings of carpet shark vertebrae produced similar results, indicating reasonable consistency (Figure 9A). Greatest mean ages recorded were 10.0 years for males and 15.5 years for females. A von Bertalanffy growth curve fitted the length-at-age data well and there was no evidence from this small sample of a difference in growth between males and females (Figure 9C). The extrapolated growth curve suggested a length at birth of about 20 cm, which is similar to the known value of 16 cm. Growth curve parameters are shown in Table 3.

Eye lens age estimates were positively correlated with TL, and there was some evidence that males were slightly older than females of the same length (Figure 9D). Eye lens age estimates were also positively correlated with mean vertebral age ($R^2 = 0.46$), but there was poor agreement between the two estimates: lens age estimates were much lower than vertebral band estimates (regression slope = 0.19). If micro-increments are formed daily, with 365 comprising one year of growth, then each vertebral band represents only 0.19 years; conversely, if vertebral bands are formed annually, micro-increments are formed every 5.3 days.

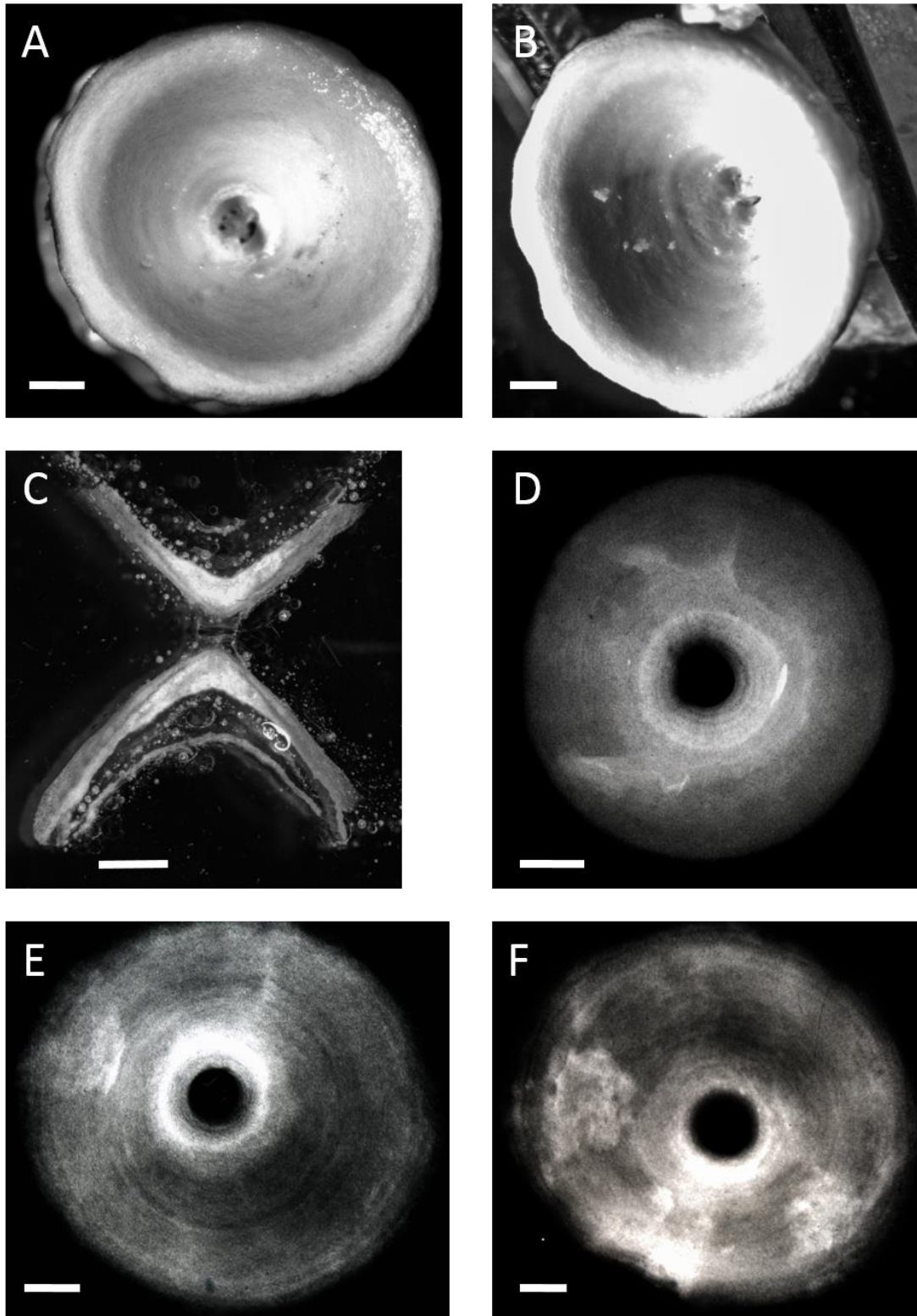


Figure 8: Images of carpet shark vertebrae. A, B: CAR 62, 76 cm TL female, whole centrum, reflected white light. C: CAR 28, unmeasured female, thick section of centrum, reflected white light. D: CAR 102, 63 cm TL female, half centrum, X-ray. E: CAR 123, 88 cm TL female, half centrum, X-ray. F: CAR 214, 87 cm TL female, half centrum, X-ray. Scale bars = 1 mm.

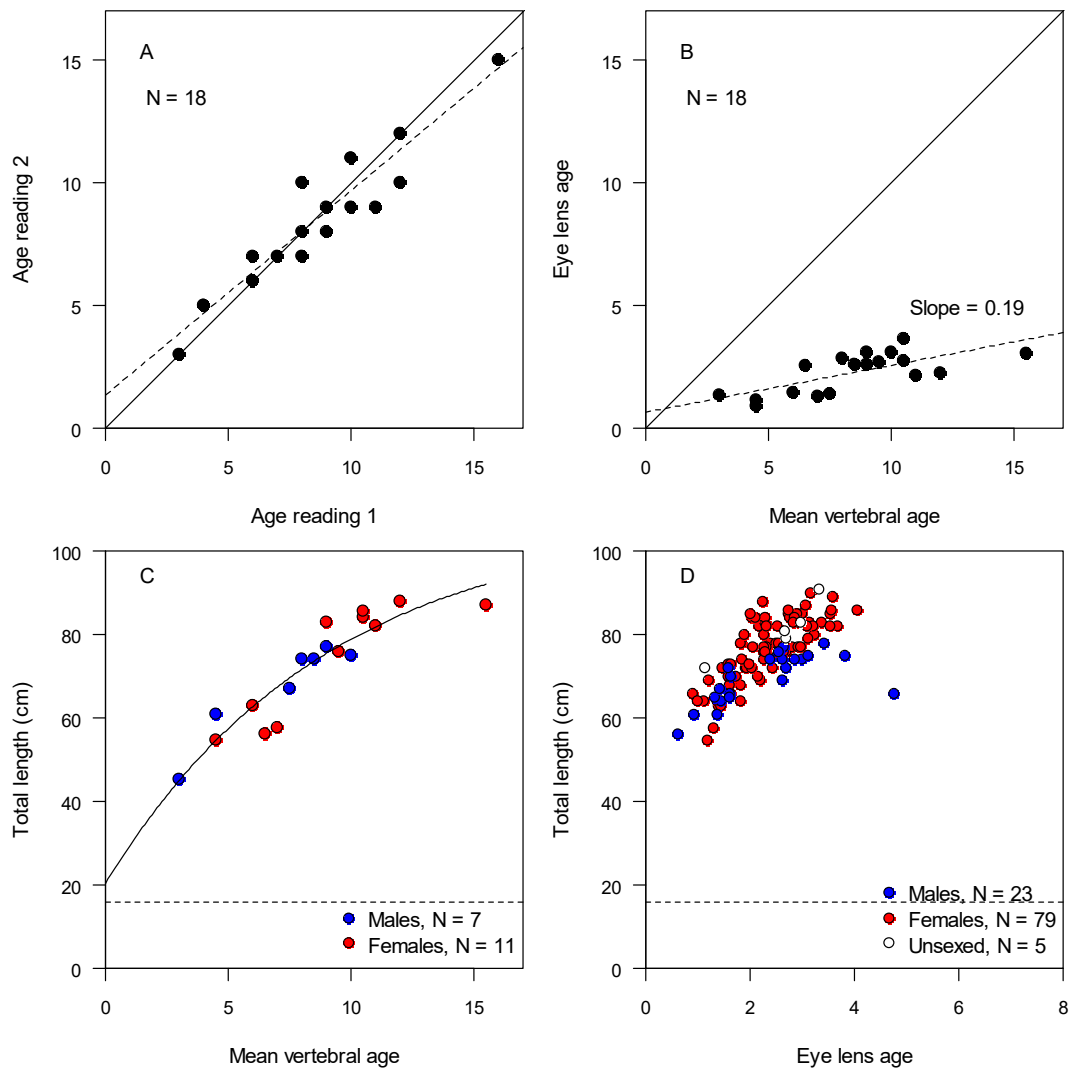


Figure 9: Age and growth estimates for carpet shark. A: Comparison of vertebral age readings 1 and 2. The solid line is the 1:1 line and the dashed line is a linear regression fitted to the data. B: Comparison of eye lens age estimate and mean vertebral age. The solid line is the 1:1 line and the dashed line is a linear regression fitted to the data. C: Plot of shark length versus mean vertebral age with fitted von Bertalanffy growth curve. The dashed line is the length at birth. D: Plot of shark length versus eye lens age. The dashed line is the length at birth.

Table 3: Growth and maturity estimates for carpet shark (CAR), common electric ray (ERA) and blind electric ray (BER). The first three rows are the von Bertalanffy growth parameters.

	Species		
	CAR	ERA	BER
L_{inf}	108.0	141.4*	44.6
K	0.110	0.128	0.154
t_0	-1.897	-0.958	-2.152
Maximum age of males (yr)	10.0	5.5	9.5
Maximum age of females (yr)	15.5	10.0	13.0
Length at 50% maturity males (cm)	60.3	44*	19.9
Length at 50% maturity females (cm)	76.1	NA	21.2
Age at 50% maturity males (yr)	5.5	2.0	1.7
Age at 50% maturity females (yr)	9.2	NA	2.0

* Pelvic length

3.4.3 Reproduction

Staged samples of carpet shark were adequate for estimating length at maturity (181 males and 179 females). There was a clear length-progression from stage 1 to stage 3 for both sexes (Figure 10). Small numbers of mature females in stage 4 (carrying uterine egg cases) and stage 6 (post-partum with distended uteri) were found and had similar lengths to stage 3 females (mature but without uterine eggs or uterus expansion). Maturity ogives fitted the data well and had tight 95% confidence intervals (Figure 10). Estimated lengths at 50% maturity were 60.3 cm (95% c.i.: 58.6–61.9) for males and 76.1 cm (95% c.i.: 74.2–77.9) for females (Table 3). Corresponding ages at maturity calculated from the von Bertalanffy growth curve in Figure 9C were 5.5 years for males and 9.2 years for females.

The number of uterine egg cases present in mature females was recorded during two research voyages, kah9306 to ECSI in May–June 1993 and kah1703 to WCSI in March–April 2017. The number of egg cases was always zero or 2 (1 per uterus). The WCSI survey had 10 sharks with zero uterine eggs, and 12 sharks with 2 uterine eggs. The ECSI survey had 8 sharks with zero uterine eggs, and 6 sharks with 2 uterine eggs. Although these sample sizes are small, they suggest that about half of the mature females are carrying uterine eggs in late summer to early winter, and that egg laying occurs during that period. In captivity, egg laying has been observed in January, May, August, November and December (E. Howard, Island Bay Marine Education Centre, Wellington, pers. comm.), suggesting that laying may occur year-round. However, this does not rule out the possibility that there is a seasonal cycle in laying intensity.

Four carpet shark eggs were laid in captivity in mid-December 2014, and they experienced ambient seawater temperatures until hatching between 10 December 2015 and 15 February 2016 (E. Howard, pers. comm.). These eggs therefore hatched after 12–14 months. One of the newly hatched young measured 17.4 cm TL. This is consistent with an observation by Waite (1909) of a 16.2 cm carpet shark escaping from an egg case when it was placed in formalin.

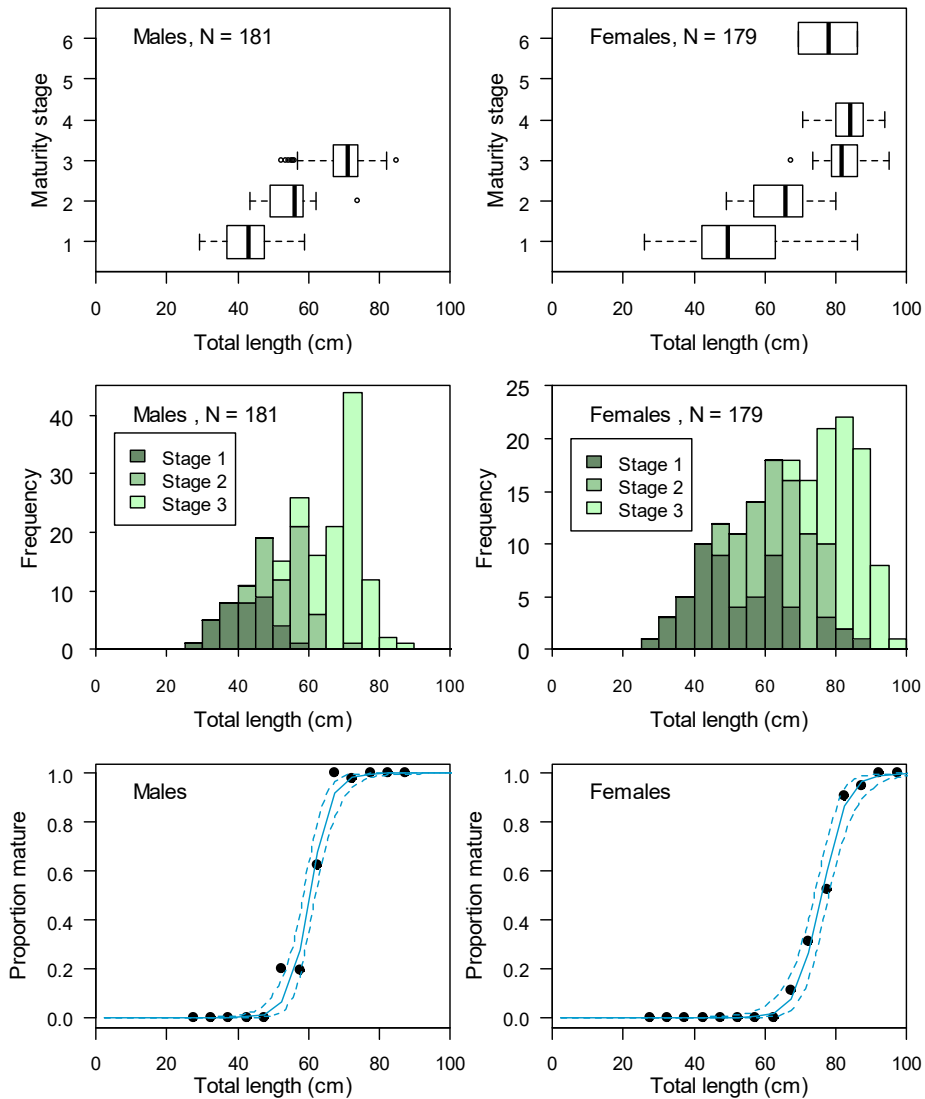


Figure 10: Maturity of male (left) and female (right) carpet sharks. Top panels: Box plots of total length classified by maturity stage (Stages 3 and above are mature individuals, see Appendix 1 for stage descriptions). The central black bar is the median, the box spans the first to third quartiles, and the whiskers extend to the most extreme data point, which is no more than 1.5 times the interquartile range from the box. Middle panels: Length-frequency distributions classified by maturity stage. For females, stage 3 combines stages 3–6. Bottom panels: Proportion of sharks that were mature (in 5 cm length intervals) with fitted logistic regression curves. Dashed lines are 95% prediction confidence intervals (± 2 standard errors).

3.5 Common electric ray (ERA)

3.5.1 Introduction

Until recently, the New Zealand common electric ray was regarded as an endemic species, *Torpedo fairchildi* (Duffy 2003b; McMillan et al. 2011; Francis 2012). Last and Stewart (2015b) reassigned the species to the genus *Tetronarce*, and noted that it is not genetically distinct from some other species in the genus. de Carvalho et al. (2016) have now synonymised the New Zealand *Tetronarce fairchildi* and the Australian *T. macneilli* with the eastern Atlantic *T. nobiliana*. Thus, the New Zealand ray should now be called *Tetronarce nobiliana*.

No studies have been carried out on the age and growth of *T. nobiliana* in New Zealand or Australia. However, *T. nobiliana* from Turkey, and two related species (*Tetronarce californica* and *Torpedo marmorata*), have been aged from their vertebrae (either whole or sectioned) (Neer & Cailliet 2001; Duman & Baştusta 2013; Kaya & Baştusta 2016; Baştusta et al. 2017).

Information about reproduction of *Tetronarce nobiliana* is sparse. Last & Stevens (2009) reported that males mature at about 52 cm TL and females mature at 62 cm TL in Australia. However, Gomon et al. (2008) and de Carvalho et al. (2016) stated that male maturity occurs at 60 cm TL in southern Australia and the ‘South Pacific’ (presumably Australia/New Zealand), meaning that length at maturity is similar in both sexes. Litter size has rarely been reported for this species. A pregnant 91 cm common electric ray (misidentified as a blind electric ray) from Otago waters had eight embryos about 7.5 cm long (Graham 1956), but it is not clear whether the female’s size was total length or disc width. Litter size is said to be as high as 60 pups in the Atlantic Ocean, with pups born at about 23 cm TL after a gestation period of about one year (Michael 1993; McEachran & de Carvalho 2002; Capapé et al. 2006; de Carvalho et al. 2016).

3.5.2 Age and growth

Common electric rays are only occasionally caught, and are not usually measured aboard research trawl surveys, or by observers. Consequently, a survey-based length-frequency distribution is not available, and our sample size in the present study was too low to do much better (Figure 1).

Common electric ray vertebrae have growth bands on the surface of the centra cones, when viewed under reflected and transmitted white light (Figure 11). These bands were judged to be clear enough without further preparation (e.g., X-raying), so they were counted and used as age estimates. Micro-CT imaging was a useful comparative tool and aid for band interpretation.

An initial plot of length versus age showed that a growth curve fitted to the data would cut the Y-axis well above the length at birth. This suggested that our band counts had included the birth band, which is not surprising as we had no newborn young or full-term embryos in our sample from which to determine the location of the birth band. Therefore, all age estimates were adjusted downwards by subtracting one. The repeat readings of common electric ray vertebrae produced similar results, indicating reasonable consistency (Figure 12A). Greatest mean ages recorded were 5.5 years for males and 10.0 years for females (Table 3), however our sample size was very small, so these values probably underestimate maximum age, especially for males as the largest male aged was only 73 cm PL. A von Bertalanffy growth curve fitted the length-at-age data well and there was no evidence from this small sample of a difference in growth between males and females (Figure 12C). The extrapolated growth curve intersected the Y-axis at almost exactly the length at birth of about 17 cm PL (estimated as 0.73×23 cm TL). Growth curve parameters are shown in Table 3.

Eye lens age estimates were positively correlated with TL, but there was considerable variability (Figure 12D). Eye lens age estimates were also positively correlated with mean vertebral age ($R^2 = 0.21$), but there was poor agreement between the two estimates: lens age estimates were much lower than vertebral band estimates (regression slope = 0.167). If micro-increments are formed daily, with 365 comprising

one year of growth, then each vertebral band represents only 0.167 years; conversely, if vertebral bands are formed annually, micro-increments are formed every 6.0 days.

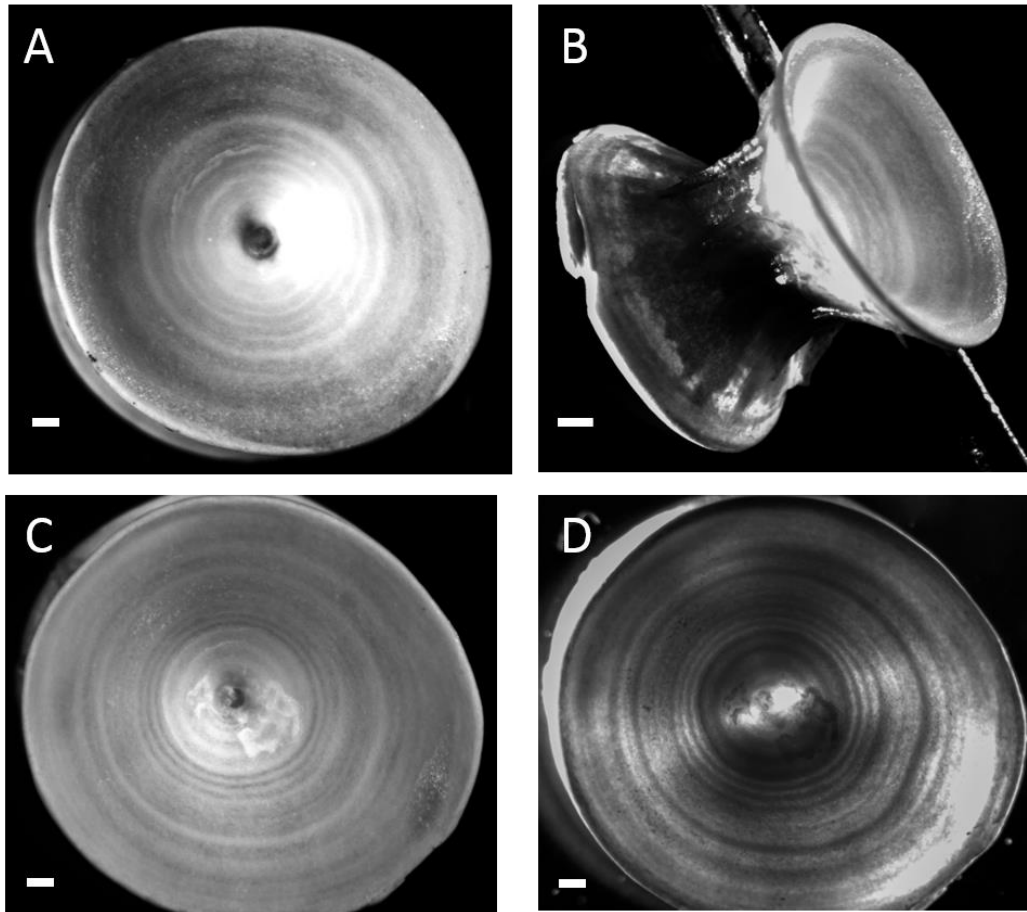


Figure 11: Images of common electric ray vertebrae. A, B: ERA 277, 109 cm PL female, whole centrum, reflected white light. C, D: ERA 301, 103 cm PL female, whole centrum, reflected and transmitted white light. Scale bars = 1 mm.

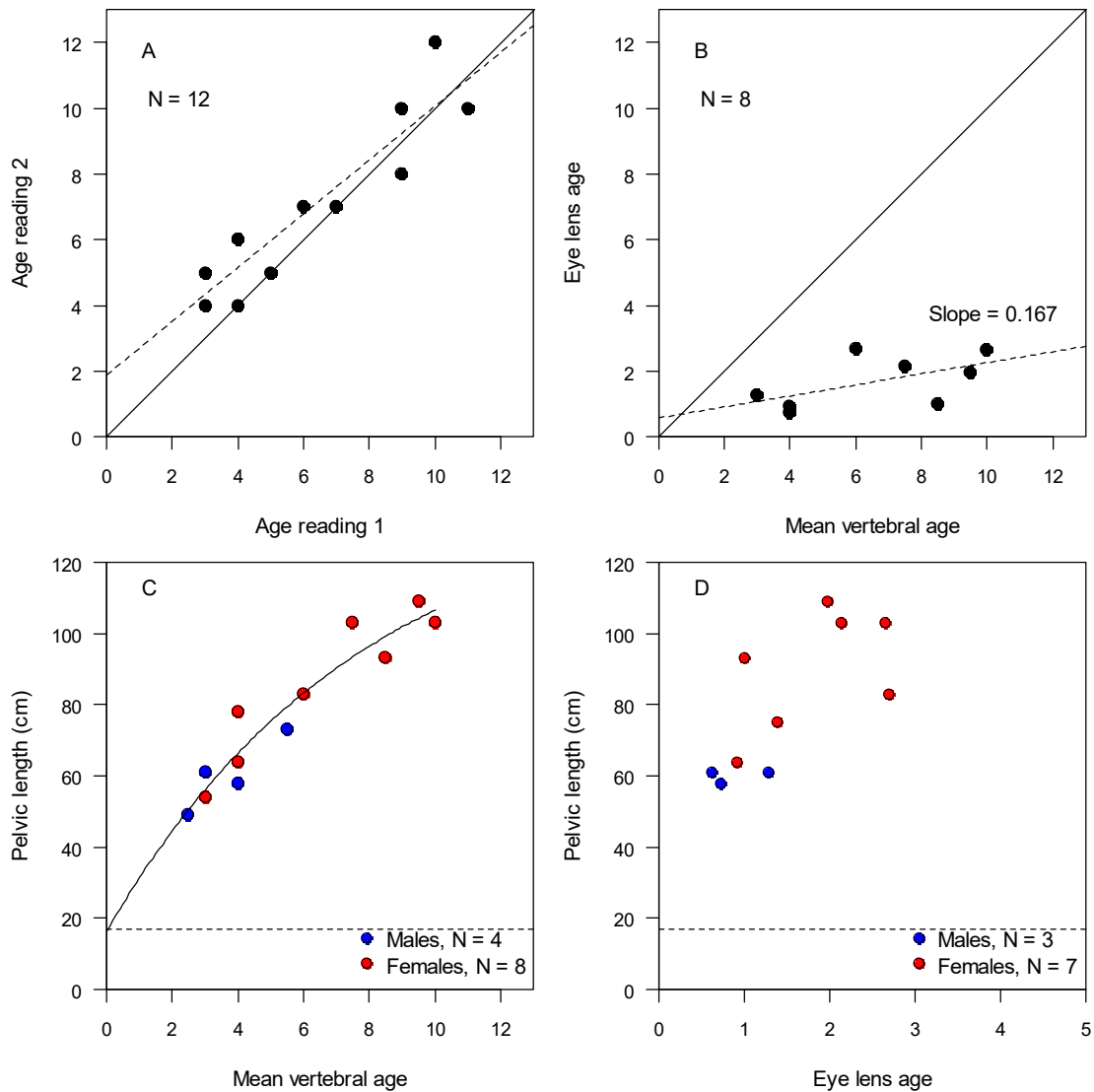


Figure 12: Age and growth estimates for common electric ray. A: Comparison of vertebral age readings 1 and 2. The solid line is the 1:1 line and the dashed line is a linear regression fitted to the data. B: Comparison of eye lens age estimate and mean vertebral age. The solid line is the 1:1 line and the dashed line is a linear regression fitted to the data. C: Plot of ray length versus mean vertebral age with fitted von Bertalanffy growth curve. The dashed line is the length at birth. D: Plot of ray length versus eye lens age. The dashed line is the length at birth.

3.5.3 Reproduction

Only a few common electric rays were staged in this study. Two males (one estimated¹ 36 cm PL (49 cm TL), the other 41 cm PL (56 cm TL)) were maturing whereas an estimated 42 cm PL (58 cm TL) male was mature. A 59 cm PL (81 cm TL) female was maturing and a 73 cm PL (103 cm TL) female was post-partum (stage 6). The 59 cm PL maturing female had clear, pink, ovarian ova with a maximum diameter of 8–10 mm, and a uterine width of 10 mm, so it had not reached full maturity. These very limited data suggest that males may mature at about 40–45 cm PL (about 55–62 cm TL) and females at 65–70 cm PL (90–95 cm TL). These estimates are consistent with a 60 cm TL at maturity of males, but not with the c. 60 cm TL at maturity for females, noted in Section 3.5.1. It is unknown whether the 59 cm PL female was late-maturing compared with other females, or whether New Zealand common electric rays mature at a larger size than Australian rays.

Based on a length at maturity of 44 cm PL (60 cm TL), males are estimated to reach maturity at 2.0 years. If female length at maturity is 45 cm PL (62 cm TL), they also mature at about 2.0 years. However, if female maturity is much larger, i.e., 65–70 cm PL (90–95 cm TL) as indicated above, the estimated age at maturity doubles to about 3.9–4.4 years. Better estimates of length and age at maturity of females are required, and results from this study are therefore not reported in Table 3.

No new data on length at birth or litter size were collected during the study.

3.6 Blind electric ray (BER, TAY, TTA)

3.6.1 Introduction

Two species of blind electric ray have been described from New Zealand: *Typhlonarke aysoni* (Hamilton 1902) and *T. tarakea* Phillipps 1929. Both species are endemic to New Zealand, and they are members of the ray Family Narkidae (Last & Stewart 2015a). The two species have been distinguished from each other by the shape of the disc (circular versus elongate/oval), disc thickness, and the length and shape of the pelvic fins (reaching or not reaching the disc margin) (Last & Stewart 2015a). However, these characters have proven difficult to determine, leading some authors to suggest that the two species may be conspecific (Ford et al. 2015; Last & Stewart 2015a). The recently published and authoritative *Rays of the World* treated *T. tarakea* as a synonym of *T. aysoni*, but provided no data to support that conclusion (de Carvalho 2016).

In a companion study (M. Francis, unpublished data), we used several sources of information to determine whether there are one or two species of *Typhlonarke*. This is an important question for the present study because it would be inappropriate to combine samples from two different species when estimating growth and reproductive parameters; similarly, it would be misleading and inefficient (in terms of sample size) to analyse two datasets separately if they represent just one species. The following analyses were carried out:

1. Thirty morphological measurements, plus weight, were recorded for 62 specimens collected around New Zealand. Data were analysed using plots of each measurement against total length, and principal components analyses.
2. Counts were made of total and monospondylous vertebrae from X-rays of 12 specimens.
3. Three mitochondrial genes (COI, ND2 and SCFD2) were sequenced from 15 specimens, and compared with three other sequences for the same genes available on Genbank.

None of the above analyses gave any indication that more than one species was represented in our samples (M. Francis, unpublished data). Our specimens covered both sexes, a wide range of sizes (including a record-sized specimen of 43.4 cm total length), and came from a broad geographical area

¹ Lengths in this paragraph were all measured unless they are shown as estimated, in which case estimates were derived from the relationship $PL = 0.73 TL$.

We therefore agree with de Carvalho (2016) that the genus *Typhlonarke* contains only one species, *T. aysoni*, and have accordingly analysed all blind electric ray data together.

There have been no previous studies on the age and growth of *Typhlonarke aysoni*, and only sparse information is available on its reproductive biology. Waite (1909) provided the first biological details based on specimens from a trawl survey of the east coast South Island in June 1907. Rays were caught between Dunedin and Foveaux Strait, and ‘many of the females contained young, eleven being the largest number obtained from an individual ... At birth ... they are ... 93 mm in length, or one-fourth that of the parent’. These numbers formed the basis for all subsequent reports of litter size and length at birth (Phillipps 1929; Cox & Francis 1997; Duffy 2003a; Last & Stewart 2015a; de Carvalho 2016). Waite also mentioned seeing embryos that were 40 mm, 50 mm and 78 mm long. Males of 35–40 cm TL were reported to be mature (de Carvalho 2016), but there is no information on the length at 50% maturity of either males or females.

Graham’s (1956) account of *T. aysoni* is unreliable because he mentions a specimen of 91 cm, which is too large to be a blind electric ray, and was obviously a misidentified common electric ray (*Tetronarce nobiliana*).

3.6.2 Age and growth

The only length-frequency distributions of blind electric rays available are based on the samples collected during the present study (Figure 1). Given the small sample sizes, there is no indication of age classes present in the length data.

Vertebrae from blind electric rays were occasionally observed to have growth bands on the surface of the centra cones, when viewed under reflected light (Figure 13A, B). However, most specimens had no visible bands, and in any event, the vertebrae were very small and would have been difficult to age under a dissecting microscope. Consequently, we X-rayed a subsample of vertebrae and used them for ageing. Growth bands were visible in most X-rays, but they were far from clear and age estimates were uncertain (Figure 13C–F). We counted these bands and used the counts as age estimates.

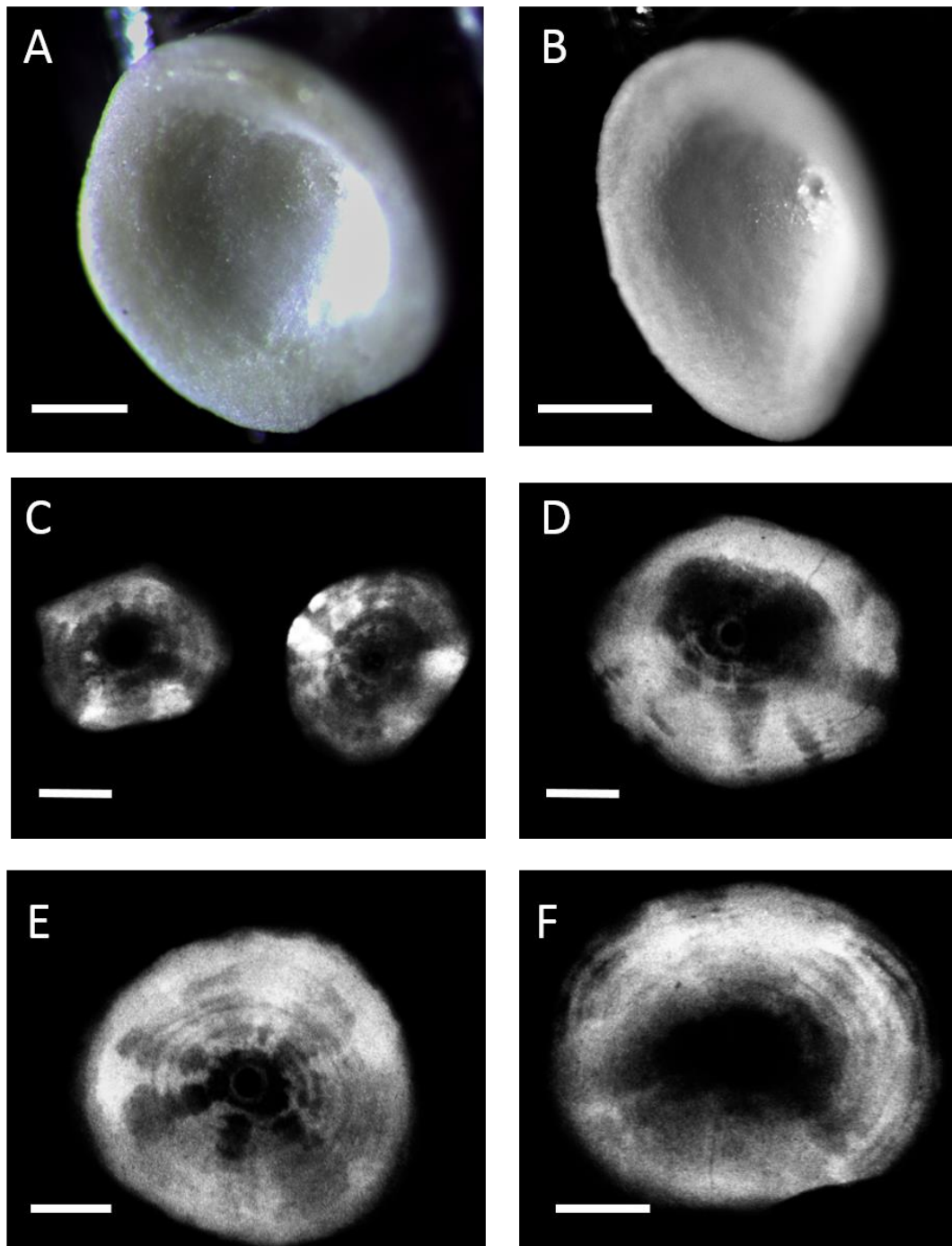


Figure 13: Images of blind electric ray vertebrae. A: BER 344, 27 cm TL female, whole centrum, reflected white light. B: BER 358, 34 cm TL female, whole centrum, reflected white light. C: BER 344, 27 cm TL female, half centrum, X-ray. D: BER 350, 35 cm TL female, half centrum, X-ray. E: BER 352, 37 cm TL female, half centrum, X-ray. F: BER 358, 34 cm TL female, half centrum, X-ray. Scale bars = 1 mm.

The repeat readings of blind electric ray vertebrae produced similar results, indicating reasonable consistency (Figure 14A). The greatest mean ages recorded were 9.5 years for males and 13.0 years for females. A von Bertalanffy growth curve fitted the length-at-age data reasonably well and there was no evidence from this small sample of a difference in growth between males and females (Figure 14B). The extrapolated growth curve suggested a length at birth of 12.6 cm TL, which is slightly greater than the estimated value of 10 cm (see Section 3.6.3). Growth curve parameters are shown in Table 3.

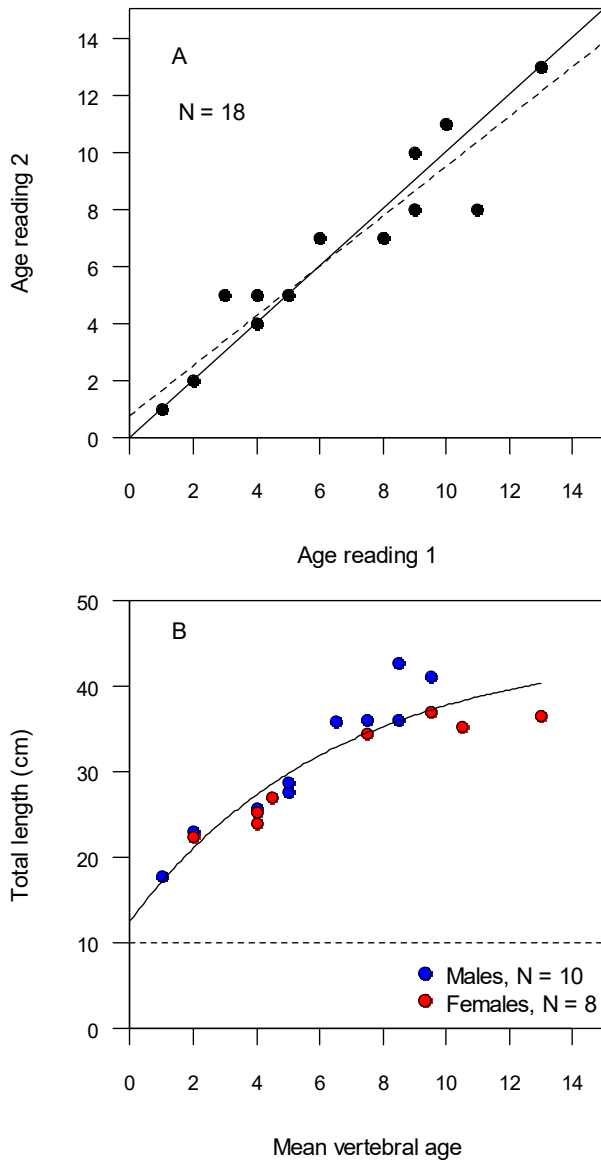


Figure 14: Age and growth estimates for blind electric ray. A: Comparison of vertebral age readings 1 and 2. The solid line is the 1:1 line and the dashed line is a linear regression fitted to the data. B: Plot of ray length versus mean vertebral age with fitted von Bertalanffy growth curve. The dashed line is the length at birth.

3.6.3 Reproduction

There was a clear length-progression from stage 1 to stage 3 for both sexes (Figure 15). Two mature females were in stage 4 (carrying uterine egg cases), nine pregnant females (stage 5) had 2–9 embryos, and eight stage 6 females (post-partum with distended uteri) had expanded, slightly bloody uteri.

Maturity ogives fitted the data moderately well, but had wide 95% prediction confidence intervals; consequently 68% prediction confidence intervals (± 1 standard error) are also shown (Figure 15). Estimated lengths at 50% maturity were 19.9 cm TL (95% c.i.: 17.3–22.5 cm) for males and 21.2 cm TL (95% c.i.: 17.5–24.9 cm) for females (Table 3). These estimates suggest that males and females mature at similar lengths, although confirmation is required when larger samples, with more individuals in the maturation range, are available. Corresponding ages at maturity calculated from the von Bertalanffy growth curve in Figure 14B were 1.7 years for males and 2.0 years for females.

Nine pregnant females were sampled (Table 4, Figure 16). They contained 2–9 embryos each, but the four smallest litters of 2–3 embryos were judged to be incomplete. Specimen 89 had two embryos in the left uterus but none in a distended right uterus, indicating recent birth or abortion of at least some of the litter. Specimens 90 and 124 had the tail of an embryo protruding from the cloaca, also suggesting possible birth or abortion of some of the litter. Thus, only the litter sizes of 5–9 are regarded as complete, although it is also possible they may not represent the full litters. Waite (1909) gave the maximum number of embryos as 11, but did not mention any other litter sizes, or state an average. Average litter size is probably fewer than 10.

Three litters of embryos smaller than 9 cm TL (specimens 86, 113 and 128) had large external yolk sacs (24–27 mm diameter), and were therefore not near full term. The other six litters had mean embryo sizes of 9.1–9.7 cm TL and the embryos had small external yolk sacs (less than 10 mm diameter) (Figure 16), indicating that they were near full term. The largest embryo measured 10.1 cm TL, and our smallest free-living juvenile was 10.5 cm TL (Figure 1). These results, in combination with the observation by Waite (1909) of near-term embryos at 9.3 cm TL having absorbed their yolk sacs, suggests that birth occurs at about 10 cm TL. The overall sex ratio in our nine litters was 18 males to 25 females. Nothing is known about the duration of the gestation period.

Table 4: Litter details for pregnant blind electric rays

Specimen	Total length of mother (cm)	Number of embryos	Sex ratio (M:F)	Embryo mean length (cm)	Embryo length range (cm)
54	36.9	7	4:3	9.1	8.9-9.5
86	33.0	6	3:3	6.8	6.6-7.1
89	30.6	2	0:2	9.1	9-9.1
90	33.2	3	1:2	9.6	9.3-10.1
99	37.8	9	7:2	9.7	9.3-9.9
113	25.7	3	0:3	8.3	8-8.6
124	25.9	2	0:2	9.6	9.4-9.8
128	23.9	5	1:4	8.1	7.8-8.4
131	30.0	6	2:4	9.2	9-9.4

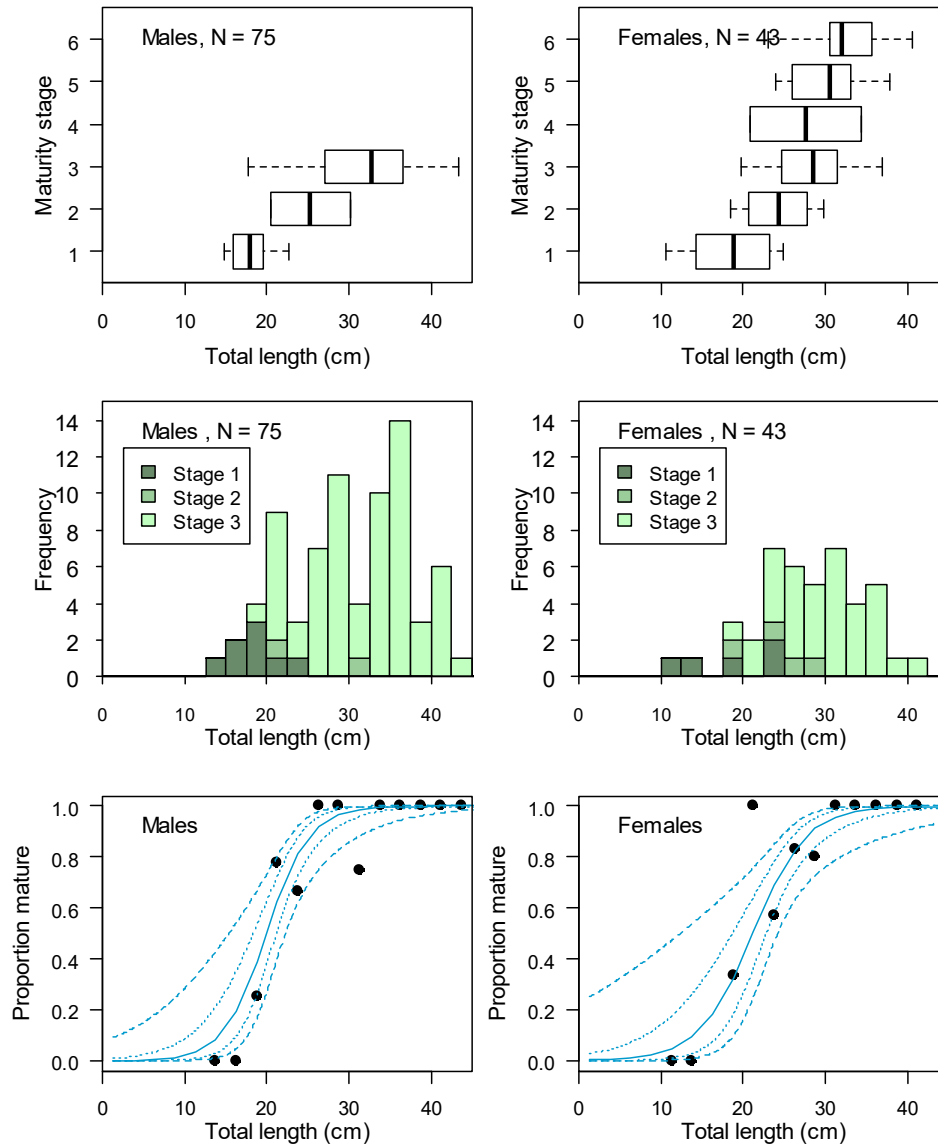


Figure 15: Maturity of male (left) and female (right) blind electric rays. Top panels: Box plots of total length classified by maturity stage (see Appendix 1 for stages). The central black bar is the median, the box spans the first to third quartiles, and the whiskers extend to the most extreme data point, which is no more than 1.5 times the interquartile range from the box. Middle panels: Length-frequency distributions classified by maturity stage. For females, stage 3 combines stages 3–6. Bottom panels: Proportion of rays that were mature (in 2.5 cm length intervals) with fitted logistic regression curves. Dashed lines are 95% prediction confidence intervals (± 2 standard errors) and dotted lines are 68% prediction confidence intervals (± 1 standard error).



Figure 16: Pregnant female blind electric ray (BER 54, 36.9 cm TL) with her seven embryos in dorsal view (top) and ventral view showing small external yolk sacs (bottom).

4. DISCUSSION

The sample sizes available for this study were small, despite having a lengthy sampling period. This partly reflects the relatively low amount of observer coverage, and few trawl surveys in shallow coastal waters where carpet shark and common electric ray are most common. It also reflects the relative rarity and/or low catchability of blind electric rays, which probably often pass through the meshes or underneath the groundlines of commercial trawl nets.

The number of specimens available for estimating age and growth was further impacted by the failure of simple methods (e.g., viewing whole cleaned vertebrae under reflected light) to reveal vertebral growth bands, and the need to resort to more complicated, time-consuming and expensive methods (e.g., X-raying, micro-CT scanning and eye lens ageing). Sample sizes suffered further attrition as a result of occasional species misidentification by observers, missing length and/or sex data, damage of specimens during preparation, and an inability to count bands on some vertebrae.

However, the biggest obstacle affecting the success of this study was the poor clarity of vertebral growth bands, even when vertebrae were X-rayed or micro-CT scanned. Common electric ray had the clearest vertebral bands, and could be aged from whole vertebrae under reflected and transmitted white light. But X-rays of carpet shark and blind electric ray were fuzzy and the bands were difficult to count. In fact, these two species were among the most difficult we have ever attempted to age from vertebrae. Furthermore, vertebral ageing has not been independently validated for those species, although that is also true of many other elasmobranch ageing studies worldwide. Nevertheless, the results presented here are regarded as preliminary and uncertain.

The use of eye lens micro-increments to estimate age has, to our knowledge, only been reported previously for cephalopods (Baqueiro Cárdenas et al. 2011; Rodríguez-Domínguez et al. 2013), so its application here to elasmobranchs is unique. The technique relies upon an assumption that the micro-increments are formed daily, in an analogous way to daily formation of micro-increments in teleost otoliths. The only known attempt to validate the daily formation of eye lens micro-increments, in reared (known-age) juvenile *Octopus maya*, found no correlation between age and the number of increments (Rodríguez-Domínguez et al. 2013). Thus, eye lens ageing has yet to be established as a valid tool.

In this study, we found large differences between age estimates from vertebrae and eye lenses, with the former exceeding the latter by factors of five for carpet shark and six for common electric ray. Since neither eye lens ageing nor vertebral ageing has been validated for these species, we cannot say which, if either, is correct. However, the vertebral ages are regarded as more plausible for the following reasons:

1. Vertebral ageing is well established as an ageing tool for elasmobranchs, and band counts have frequently been validated as being formed annually (Cailliet & Goldman 2004; Cailliet 2015). However, there is a small but growing number of sharks for which vertebral bands are unrelated to age, are formed twice per year rather than once, or seriously and systematically underestimate age (particularly among older individuals of longer-lived species) (Natanson & Cailliet 1990; Kalish & Johnston 2001; Francis et al. 2007; Wells et al. 2013; Harry 2017).
2. Eye lens micro-increment ageing has not yet been validated for any animal, and was proven invalid for reared *Octopus maya*.
3. The ages at maturity estimated from vertebral bands were 5.5–9.2 years for carpet shark and 2.0 years for male common electric ray (Table 3). If the eye lens ages for these species were correct, the ages at maturity would reduce to 1.0–1.7 for carpet shark and 0.3 years for common electric ray. Such low ages at maturity would be extraordinary for an elasmobranch.
4. Maximum female vertebral ages were estimated to be 15.5 years for carpet shark and 10.0 years for common electric ray (though these likely underestimate the true maxima given our small sample sizes). If the eye lens ages for these species were correct, the maximum ages would reduce to 2.9 years for carpet shark and 1.7 years for common electric ray. These values imply a reproductively active period of only 1–2 years for carpet shark and 1.4 years for male common electric ray. Productivity constraints are placed on these species by their reproductive strategies: their annual fecundity, and therefore replacement rate, are low because reproduction involves the time- and energy-consuming production of large leathery egg cases or large live young. Gestation periods for viviparous rays and sharks are typically 6–15 months where they are known. It seems improbable that carpet shark and common electric ray could complete enough reproductive cycles within the reproductive lifespan implied by eye lens ageing to replace losses due to natural mortality.

This does not mean that eye lens ageing should be abandoned as an ageing tool. If there is a constant relationship, or even a quantifiable size-dependent relationship, between the number of micro-increments deposited in lenses and an animal's age, then eye lens diameters may provide a useful estimate of age. A good way to quantify the relationship would be to count micro-increments in newborn sharks or rays and, at a later date, known-age animals from the same cohort. For example, 0+ rig are born in Porirua Harbour in spring and emigrate the following autumn–winter at an age of 5–7 months (Francis & Francis 1992; Francis 2013). Differences in increment counts for 0+ rig captured in spring and autumn would provide a quick test of whether increments are formed daily or with some other

periodicity. Another test could involve the injection of a fluorescent chemical that is deposited in the eye lenses of tagged and released sharks or rays. Recapture of those animals would enable the estimation of the number of micro-increments formed between injection and recapture. This procedure would be analogous to the injection of oxytetracycline into teleosts for validating otolith growth band formation, but would use a different chemical (one that bonds to protein instead of calcium, and one that does not affect the vision of sharks and rays).

Carpet shark has not previously been aged. However, several studies on other species in the genus *Cephaloscyllium* provided estimates of growth rate, length at maturity, and longevity (reviewed by Horn 2016). *Cephaloscyllium umbratile* was observed to grow about 12 cm in its first year, which is slightly faster than the estimated first-year growth of 9 cm for carpet shark calculated from our von Bertalanffy growth curve. Bell (2012) counted zones on the surface of vertebrae of *C. albipinnum*, and estimated that they reached sexual maturity at 8–13 years and had a maximum age of c. 20 years, both of which are higher than our carpet shark estimates of 5–9 years at maturity and at least 15.5 years' maximum age. Tagged *C. laticeps* have been observed to live at least 7 years (Awruch et al. 2012). These results are consistent in suggesting that species of *Cephaloscyllium* have moderately fast growth and moderate longevity.

Virtually no biological information is available on common electric rays in New Zealand waters. However, the re-classification of this species as *Tetronarce nobiliana* enables comparison of our results with those from studies of *T. nobiliana* elsewhere. Caution is required though, because different populations may have different biological parameters. This species is currently thought to have two disjunct geographical populations: one in the eastern Atlantic Ocean and Mediterranean Sea and the other in the south-west Pacific Ocean around New Zealand and Australia (de Carvalho et al. 2016). Kaya and Başusta (2016) used sectioned and stained vertebrae to age *T. nobiliana* from Turkey. Unfortunately, their sample lacked adults, with the largest ray being 35 cm TL. These juveniles ranged from 1 to 5 years old, with 4-year-olds being about 32 cm TL and 5-year-olds 36 cm TL. Those growth rates are much lower than our estimates for New Zealand rays, which suggest they reach about 60 cm PL (c. 82 cm TL) in 4 years (Figure 12). Whether the difference reflects different vertebral preparation techniques (e.g., sectioning and staining may reveal more growth bands than does examination of whole unstained vertebrae), or population differences is unknown. A related study on growth in *Torpedo marmorata* found results similar to those for *T. nobiliana* from Turkey, with 4-year-olds being about 30 cm TL and 5-year-olds 35 cm TL with a maximum age of 6 years (Duman & Başusta 2013); however, that study also appears to have sampled only juveniles. Marginal increment analysis revealed a unimodal distribution, which the authors interpreted as validation of the annual nature of the bands they counted; however, their graph shows only the mean increment ratios with no error bars, so it is impossible to assess the veracity of their claim. Neer and Cailliet (2001) aged whole vertebrae from Californian *Torpedo californica* after enhancing the surface banding structure by 'scraping' with a soft graphite pencil. They estimated that that species matures at 6 years for males and 9 years for females, with a maximum age of 16 years; all those values are considerably greater than our estimates for *Tetronarce nobiliana*.

Some reproductive parameters have been estimated here for the first time, or revised or confirmed. Carpet shark males mature at about 60 cm TL and females at 76 cm TL. These lengths are the same as those reported by Horn (2016), which is not surprising as our dataset included all the biological data available to him, supplemented with more recently collected data. Observations during trawl surveys of females carrying uterine eggs, supplemented by observations of egg laying in captivity, indicate that egg laying occurs year-round, as also noted by Horn (2016). The time to hatching after deposition of eggs in an aquarium was about 12–14 months, although development time is almost certainly temperature-dependent as has been shown in elephantfish (*Callorhinchus milii*), which produces similar large leathery eggs that are deposited on the seabed (Lyon et al. 2011). Length at hatching is confirmed as about 16–17 cm TL.

Our samples provided few useful data on reproduction in common electric rays. The lengths at maturity reported for Australian specimens were about 60 cm TL for both sexes (see Section 3.5.1). But we note

that one of our females was not yet mature at 59 cm PL (81 cm TL). In the Mediterranean Sea, *Tetronarce nobiliana* males mature at about 55 cm TL and females at over 90 cm TL (Capapé et al. 2006), providing evidence of a substantially greater size at maturity for females than males. Females also mature at larger sizes than males in *Tetronarce californica*, *Torpedo mackayana* and *Torpedo marmorata*, but not in *Torpedo torpedo* (Capapé et al. 2001; Neer & Cailliet 2001; Consalvo et al. 2007). Other aspects of reproduction in common electric rays are totally unknown in New Zealand or Australian waters. In the Mediterranean, *T. nobiliana* females grow larger than males (120 cm TL versus 75 cm TL); gestation lasts one year and there is no concurrent ovarian egg development, suggesting that birth is followed by a resting period and that the reproductive cycle may be two years long; birth occurs at 17–22 cm TL; and fecundity increases with the size of the mother (Capapé et al. 2006). Elsewhere, litter size is said to be as high as 60 pups in the Atlantic Ocean, with pups born at about 20–25 cm (23 cm) TL after a gestation period of about one year (Michael 1993; McEachran & de Carvalho 2002; Capapé et al. 2006; de Carvalho et al. 2016). These reproductive parameters are the best available for application to the New Zealand population, but they need corroboration from further research.

Considerable new information was available on reproduction of blind electric rays. Median lengths at sexual maturity were about 20–21 cm TL for both sexes, although the confidence intervals were relatively wide because of variability in the data and small sample sizes around the maturation length range. Nine pregnant females were found, providing the first litters to be reported since Waite (1909), who recorded a litter of 11 embryos (plus others that he didn't enumerate). Four of our litters were probably incomplete, and the other five had 5–9 embryos. Litter size probably averages less than 10 embryos, with a maximum recorded of 11 (Waite 1909). The length at birth is confirmed to be 10 cm TL. No information is available on the length of the gestation period or whether females have a resting period between pregnancies. Males and females appear to reach similar maximum lengths (Figure 1), with a 43.4 cm male reported here being the largest specimen yet recorded. The previously reported maximum length was 38 cm TL based on Museum of New Zealand specimens (Last & Stewart 2015a). Recently, de Carvalho (2016) suggested they reach 45 cm TL, but apparently without any more specimens than were available to Last & Stewart (2015a).

A summary of the new age, growth and reproductive parameters obtained during the present study is given in Table 5.

Table 5: Summary of new age, growth and reproductive parameters obtained during the present study.

	Species		
	CAR	ERA	BER
L_{inf}	108.0	141.4*	44.6
K	0.110	0.128	0.154
t_0	-1.897	-0.958	-2.152
Length at birth or hatching (cm)	16.0	17*	10.0
Maximum age of males (yr)	10.0	5.5	9.5
Maximum age of females (yr)	15.5	10.0	13.0
Length at 50% maturity males (cm)	60.3	44*	19.9
Length at 50% maturity females (cm)	76.1	NA	21.2
Age at 50% maturity males (yr)	5.5	2.0	1.7
Age at 50% maturity females (yr)	9.2	NA	2.0
Gestation/hatching period (months)	12-14	NA	NA
Average litter size	NA	NA	< 10

* Pelvic length

5. MANAGEMENT IMPLICATIONS

Preliminary vertebrae-based growth curves were derived for carpet shark, common electric ray and blind electric ray. The results indicate that all three species grow moderately fast, reaching maturity at about 2 years for male common electric rays and both sexes of blind electric rays, and 5 or 9 years for male and female carpet shark, respectively. Longevity is low to moderate, compared with other elasmobranchs, being 5–10 years for males of the three species and 10–16 years for females. These estimates are uncertain and potentially inaccurate, because of the lack of ageing validation and the small sample sizes. For comparison, rig (*Mustelus lenticulatus*) is regarded as moderately productive, and it matures at 6–8 years and lives up to about 20 years (Francis & Ó Maolagáin 2000; Ford et al. 2015). If eye lens micro-increments are validated as being formed daily, the productivity of carpet shark and common electric ray would be even greater, because their growth rates would be faster and longevity lower than determined from vertebral ageing.

Our age estimates suggest that carpet shark has similar productivity to rig, and the two electric ray species are more productive than either carpet shark or rig. However, some reproductive parameters are unknown. In particular, the length of the gestation period, and whether females have a resting period between pregnancies, are unknown for the two electric rays, as is the number of eggs laid annually by carpet sharks. Uncertainty about these parameters would have a big effect on productivity estimates. For example, annual reproductive output for a species with a one-year gestation period and a one-year resting period is only 25% of that for a species with a six-month gestation period and no resting period.

6. ACKNOWLEDGMENTS

Special thanks to all the NIWA scientific staff and MPI observers who collected the data and specimens used in this study. We also thank Derek Kater for carrying out the micro-CT scans; Chris Francis for advice on R programming; Judy Sutherland for assistance with interpreting genetic data; Peter Horn for reviewing the draft report, and Rich Ford for valuable input. We are grateful to Andrew McNaughton (University of Otago) who provided access, expertise and training on the micro-CT scanner. This work was completed under Ministry for Primary Industries project ENV2014–02.

7. REFERENCES

- Abramoff, M.D.; Magalhães, P.J.; Ram, S.J. (2004). Image processing with ImageJ. *Biophotonics International* 11 (7): 36–42.
- Anderson, O.F.; Bagley, N.W.; Hurst, R.J.; Francis, M.P.; Clark, M.R.; McMillan, P.J. (1998). Atlas of New Zealand fish and squid distributions from research bottom trawls. *NIWA Technical Report* 42. 303 p.
- Awruch, C.A.; Frusher, S.D.; Stevens, J.D.; Barnett, A. (2012). Movement patterns of the draughtboard shark *Cephaloscyllium laticeps* (Scyliorhinidae) determined by passive tracking and conventional tagging. *Journal of Fish Biology* 80: 1417–1435.
- Baqueiro Cárdenas, E.R.; Medrano Correa, S.; Contreras Guzman, R.; Barahona, N.; Briceño, F.; José Villegas, M.; Paredes, R. (2011). Eye lens structure of the octopus *Enteroctopus megalocyathus*: evidence of growth. *Journal of Shellfish Research* 30: 199–204.
- Başusta, N.; Demirhan, S.A.; Çiçek, E.; Başusta, A. (2017). Comparison of staining techniques for age determination of some chondrichthyan species. *Turkish Journal of Fisheries and Aquatic Sciences* 17: 41–49.
- Bell, J.D. (2012). Reproduction and ageing of Australian holocephalans and white-fin swell shark. PhD Thesis, Deakin University, Victoria, Australia. 178 p.
- Cailliet, G.M. (2015). Perspectives on elasmobranch life-history studies: a focus on age validation and relevance to fishery management. *Journal of Fish Biology* 87: 1271–1292.

- Cailliet, G.M.; Goldman, K.J. (2004). Age determination and validation in chondrichthyan fishes. *In*: Carrier, J.C.; Musick, J.A.; Heithaus, M.R. (eds). The biology of sharks and their relatives. pp 399–447. CRC Press, Boca Raton, Florida.
- Capapé, C.; Guélorget, O.; Vergne, Y.; Quignard, J.-P.; Ben Amor, M.M.; Bradai, M.N. (2006). Biological observations on the black torpedo, *Torpedo nobiliana* Bonaparte 1835 (Chondrichthyes: Torpedinidae), from two Mediterranean areas. *Annales Series Historia Naturalis* 16: 19–28.
- Capapé, C.; Seck, A.A.; Diatta, Y.; Diop, M. (2001). Observations on the reproductive biology of *Torpedo (Tetronarce) mackayana* (Torpedinidae), from the coast of Senegal (eastern tropical Atlantic). *Cybium* 25: 95–99.
- Consalvo, I.; Scacco, U.; Romanelli, M.; Vacchi, M. (2007). Comparative study on the reproductive biology of *Torpedo torpedo* (Linnaeus, 1758) and *T. marmorata* (Risso, 1810) from the central Mediterranean Sea. *Scientia Marina* 7: 213–222.
- Cox, G.; Francis, M. (1997). Sharks and rays of New Zealand. Canterbury University Press, Christchurch. 68 p.
- Crivelli, A. (1980). The eye lens weight and age in the common carp, *Cyprinus carpio* L. *Journal of Fish Biology* 16: 469–473.
- de Carvalho, M.R. (2016). Sleeper rays. Family Narkidae. *In*: Last, P.; White, W.; de Carvalho, M.; Séret, B.; Stehmann, M.; Naylor, G. (eds). Rays of the world. pp 170–181. CSIRO Publishing, Clayton South, Victoria, Australia.
- de Carvalho, M.R.; Last, P.R.; Séret, B. (2016). Torpedo rays. Family Torpedinidae. *In*: Last, P.; White, W.; de Carvalho, M.; Séret, B.; Stehmann, M.; Naylor, G. (eds). Rays of the world. pp 184–203. CSIRO Publishing, Clayton South, Victoria, Australia.
- Douglas, R.H. (1987). Ocular lens diameter as an indicator of age in brown trout, *Salmo trutta*. *Journal of Fish Biology* 31: 835–836.
- Duffy, C.A.J. (2003a). Blind electric ray *Typhlonarke aysoni* (Hamilton 1902) and oval electric ray *Typhlonarke tarakea* Phillipps 1929. *In*: Cavanagh, R.D.; Kyne, P.M.; Fowler, S.L.; Musick, J.A.; Bennett, M.B. (eds). The conservation status of Australasian chondrichthyans: report of the IUCN Shark Specialist Group Australia and Oceania Regional Red List Workshop. pp 138, School of Biomedical Sciences, University of Queensland, Brisbane.
- Duffy, C.A.J. (2003b). New Zealand torpedo rays *Torpedo fairchildi* Hutton, 1872. *In*: Cavanagh, R.D.; Kyne, P.M.; Fowler, S.L.; Musick, J.A.; Bennett, M.B. (eds). The conservation status of Australasian chondrichthyans: report of the IUCN Shark Specialist Group Australia and Oceania Regional Red List Workshop. pp 139–140, School of Biomedical Sciences, University of Queensland, Brisbane.
- Duman, O.V.; Başusta, N. (2013). Age and growth characteristics of marbled electric ray *Torpedo marmorata* (Risso, 1810) inhabiting Iskenderun Bay, north-eastern Mediterranean Sea. *Turkish Journal of Fisheries and Aquatic Sciences* 13: 541–549.
- Fernald, R.D. (1985). Growth of the teleost eye: novel solutions to complex constraints. *Environmental Biology of Fishes* 13: 113–123.
- Ford, R.B.; Galland, A.; Clark, M.R.; Crozier, P.; Duffy, C.A.J.; Dunn, M.; Francis, M.P.; Wells, R. (2015). Qualitative (Level 1) risk assessment of the impact of commercial fishing on New Zealand chondrichthyans. *New Zealand Aquatic Environment and Biodiversity Report No. 157*. 111 p.
- Francis, M. (2012). Coastal fishes of New Zealand. Fourth edition. Craig Potton Publishing, Nelson. 268 p.
- Francis, M.P. (2013). Temporal and spatial patterns of habitat use by juveniles of a small coastal shark (*Mustelus lenticulatus*) in an estuarine nursery. *PLoS ONE* 8 (2): e57021: 1–15.
- Francis, M.P.; Campana, S.E.; Jones, C.M. (2007). Age under-estimation in New Zealand porbeagle sharks (*Lamna nasus*): is there an upper limit to ages that can be determined from shark vertebrae? *Marine and Freshwater Research* 58: 10–23.
- Francis, M.P.; Francis, R.I.C.C. (1992). Growth rate estimates for New Zealand rig (*Mustelus lenticulatus*). *Australian Journal of Marine and Freshwater Research* 43: 1157–1176.

- Francis, M.P.; Jones, E.; Ó Maolagáin, C.; Lyon, W.S. (2018). Growth and reproduction of four deepwater sharks in New Zealand waters. *New Zealand Aquatic Environment and Biodiversity Report No. 196*. 56 p.
- Francis, M.P.; Ó Maolagáin, C. (2000). Age, growth and maturity of a New Zealand endemic shark (*Mustelus lenticulatus*) estimated from vertebral bands. *Marine and Freshwater Research* 51: 35–42.
- Francis, M.P.; Ó Maolagáin, C. (2001). Development of ageing techniques for dark ghost shark (*Hydrolagus novaezelandiae*). Final Research Report for Ministry of Fisheries Research Project MOF2000/03C. 17 p.
- Garrick, J.A.F. (1951). The blind electric rays of the genus *Typhlonarke* (Torpedinidae). Zoology publications from Victoria University College 15. 6 p.
- Garrick, J.A.F. (1952). The systematics and some aspects of the anatomy of the New Zealand blind electric rays of the G. *Typhlonarke* (Torpedinidae). MSc Thesis, Victoria University of Wellington, Wellington. 135 p.
- Geraghty, P.T.; Jones, A.S.; Stewart, J.; Macbeth, W.G. (2012). Micro-computed tomography: an alternative method for shark ageing. *Journal of Fish Biology* 80: 1292–1299.
- Gomon, M.F.; Bray, D.J.; Kuitert, R.H. (2008). Fishes of Australia's southern coast. Reed New Holland, Sydney. 928 p.
- Graham, D.H. (1956). A treasury of New Zealand fishes. Second edition. Reed, Wellington. 424 p.
- Harry, A.V. (2017). Evidence for systemic age underestimation in shark and ray ageing studies. *Fish and Fisheries*. doi: 10.1111/faf.12243.
- Horn, P.L. (2016). Biology of the New Zealand carpet shark *Cephaloscyllium isabellum* (Scyliorhinidae). *Journal of Ichthyology* 56: 336–347.
- Kalish, J.; Johnston, J. (2001). Determination of school shark age based on analysis of radiocarbon in vertebral collagen. In: Kalish, J.M. (ed) Use of the bomb radiocarbon chronometer to validate fish age. pp 116–129, Final Report FRDC Project 93/109. Fisheries Research and Development Corporation, Canberra, Australia.
- Kaya, G.; Başusta, N. (2016). A study on age and growth of juvenile and semi adult *Torpedo nobiliana* Bonaparte, 1835 inhabiting Iskenderun Bay, northeastern Mediterranean Sea. *Acta Biologica Turcica* 29: 143–149.
- Last, P.R.; Stevens, J.D. (2009). Sharks and rays of Australia. Second edition. CSIRO, Hobart. 644 p.
- Last, P.R.; Stewart, A.L. (2015a). Family Narkidae. In: Roberts, C.D.; Stewart, A.L.; Struthers, C.D. (eds). The fishes of New Zealand. pp 172–174, Te Papa Press, Wellington.
- Last, P.R.; Stewart, A.L. (2015b). Family Torpedinidae. In: Roberts, C.D.; Stewart, A.L.; Struthers, C.D. (eds). The fishes of New Zealand. pp 169–171, Te Papa Press, Wellington.
- Lyon, W.S.; Francis, R.I.C.C.; Francis, M.P. (2011). Calculating incubation times and hatching dates for embryonic elephantfish (*Callorhynchus milii*). *New Zealand Journal of Marine and Freshwater Research* 45: 59–72.
- McEachran, J.D.; de Carvalho, M.R. (2002). Batoid fishes. In: Carpenter, K.E. (ed) FAO species identification guide for fishery purposes. The living marine resources of the western central Atlantic. Volume 1 Introduction, molluscs, crustaceans, hagfishes, sharks, batoid fishes and chimaeras. pp 507–589, FAO, Rome.
- McMillan, P.J.; Francis, M.P.; James, G.D.; Paul, L.J.; Marriott, P.J.; Mackay, E.; Wood, B.A.; Griggs, L.H.; Sui, H.; Wei, F. (2011). New Zealand fishes. Volume 1: A field guide to common species caught by bottom and midwater fishing. *New Zealand Aquatic Environment and Biodiversity Report No. 68*. 329 p.
- Michael, S.W. (1993). Reef sharks and rays of the world. A guide to their identification, behavior, and ecology. Sea Challengers, Monterey, California. 107 p.
- Ministry for Primary Industries. (2013). National plan of action for the conservation and management of sharks 2013. Ministry for Primary Industries, Wellington. 32 p.
- Nakaya, K.; Sato, K.; Kawachi, J.; Stewart, A.L. (2015). Family Scyliorhinidae. In: Roberts, C.D.; Stewart, A.L.; Struthers, C.D. (eds). The fishes of New Zealand. pp 75–89. Te Papa Press, Wellington.
- Natanson, L.J.; Cailliet, G.M. (1990). Vertebral growth zone deposition in Pacific angel sharks. *Copeia* 1990: 1133–1145.

- Neer, J.A.; Cailliet, G.M. (2001). Aspects of the life history of the Pacific electric ray, *Torpedo californica* (Ayres). *Copeia* 2001 (3): 842–847.
- Phillipps, W.J. (1929). Elasmobranch fishes of New Zealand: No. 3. *New Zealand Journal of Science and Technology* 11: 98–107.
- R Development Core Team. (2008). R: A language and environment for statistical computing. <http://www.R-project.org>. R Foundation for Statistical Computing, Vienna, Austria. p.
- Rodríguez-Domínguez, A.; Rosas, C.; Méndez-Loeza, I.; Markaida, U. (2013). Validation of growth increments in stylets, beaks and lenses as ageing tools in *Octopus maya*. *Journal of Experimental Marine Biology and Ecology* 44: 194–199.
- Siezen, R.J. (1989). Eye lens ageing in the spiny dogfish (*Squalus acanthias*). I. Age determination from lens weight. *Current Eye Research* 8: 707–712.
- Tanaka, S. (1990). Age and growth studies on the calcified structures of newborn sharks in laboratory aquaria using tetracycline. *NOAA Technical Report NMFS* 90: 189–202.
- Taniuchi, T. (1988). Aspects of reproduction and food habits of the Japanese swellshark *Cephaloscyllium umbratile* from Choshi, Japan. *Nippon Suisan Gakkaishi* 54: 627–633.
- Waite, E.R. (1909). Scientific results of the New Zealand Government trawling expedition, 1907. Government Printer, Wellington. 116 p.
- Wells, R.J.D.; Smith, S.E.; Kohin, S.; Freund, E.; Spear, N.; Ramon, D.A. (2013). Age validation of juvenile shortfin mako (*Isurus oxyrinchus*) tagged and marked with oxytetracycline off southern California. *Fishery Bulletin* 111: 147–160.
- Wilson, C.A.; Beamish, R.J.; Brothers, E.B.; Carlander, K.D.; Casselman, J.M.; Dean, J.M.; Jearld, A.; Prince, E.D.; Wild, A. (1987). Glossary. In: Summerfelt, R.C.; Hall, G.E. (eds). Age and growth of fish. pp 527–529, Iowa State University Press, Ames, USA.

APPENDIX 1: Reproductive staging guide for sharks and rays

Stage	Name	Males	Females
1	Immature	Claspers shorter than pelvic fins, soft and uncalcified, unable or difficult to splay open.	Ovaries small and undeveloped. Oocytes not visible, or small (pin-head sized) and translucent whitish.
2	Maturing	Claspers longer than pelvic fins, soft and uncalcified, unable or difficult to splay open or rotate forwards.	Some oocytes enlarged, up to about pea-sized or larger, and white to cream.
3	Mature	Claspers longer than pelvic fins, hard and calcified, able to splay open and rotate forwards to expose clasper spine.	Some oocytes large (greater than pea-sized) and yolky (bright yellow).
4	Gravid I	<i>Not applicable</i>	Uteri contain eggs or egg cases but no embryos are visible.
5	Gravid II	<i>Not applicable</i>	Uteri contain visible embryos. <i>Not applicable to egg-laying sharks and skates.</i>
6	Post-partum	<i>Not applicable</i>	Uteri flaccid and vascularised indicating recent birth.